Altering The Electrochromic Parameters Of All-Organic Device By The Doping Of Different Metal Oxides

M.Sc. Thesis

By
MD SAHID AHMED

DEPARTMENT OF PHYSICS
INDIAN INSTITUTE OF TECHNOLOGY INDORE
May, 2024

Altering The Electrochromic Parameters Of All-Organic Device By The Doping Of Different Metal Oxides

A THESIS

Submitted in partial fulfillment of the requirements for the award of the degree
of
Master of Science

by
MD SAHID AHMED

DEPARTMENT OF PHYSICS
INDIAN INSTITUTE OF TECHNOLOGY INDORE
May, 2024

INDIAN INSTITUTE OF TECHNOLOGY INDORE

CANDIDATE'S DECLARATION

I hereby certify that the work which is being presented in the thesis entitled **Altering The Electrochromic Parameters Of All-Organic Device By The Doping Of Different Metal Oxides**, in the partial fulfillment of the requirements for the award of the degree of **MASTER OF SCIENCE** and submitted in the **DEPARTMENT OF PHYSICS, Indian Institute of Technology Indore**, is an authentic record of my own work carried out during the time period from June 2023 to May 2024 under the supervision of **Prof. Rajesh Kumar**, Professor, IIT Indore.

The matter presented in this thesis has not been submitted by me for the award of any other degree of this or any other institute.

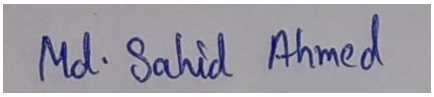

Signature of the student with date
MD SAHID AHMED

This is to certify that the above statement made by the candidate is correct to the best of my/our knowledge.

Signature of the Supervisor of
M.Sc. thesis
(Prof. RAJESH KUMAR)

MD SAHID AHMED has successfully given her M.Sc. Oral Examination held on **16th May 2024.**

Signature of Supervisor of MSc thesis
Date: 22/05/2024

Convener, DPGC
Date: 22/05/2024

ACKNOWLEDGEMENTS

I extend my sincere gratitude to Professor Rajesh Kumar for his invaluable guidance and unwavering support throughout this research journey. His mentorship has been instrumental in shaping my understanding and approach towards electrochromic materials.

I am indebted to Bhumika Sahu for her role as both a mentor and a friend. Her insightful advice and encouragement have been a source of motivation at every step of this endeavor.

I would like to express my appreciation to Shivansh Raj Pandey for his companionship and unwavering emotional support, even if it came with a fair share of time-wasting moments.

Special thanks to Dr. Tanushree Ghosh for generously allowing me to utilize her schematics, which significantly enriched the quality of my work.

To my friends, whose unique blend of sarcasm and humor has kept me grounded throughout this journey, thank you for providing occasional distractions and moments of levity amidst the seriousness of research.

Lastly, I am grateful to all my lab-mates for their direct and indirect contributions, specifically Deb Kumar Rath for Raman Spectroscopy, Love Bansal for discussion, Nikita Ahlawat for her home made food, which have collectively contributed to the success of this project.

Md Sahid Ahmed

Master of Science

Department of Physics

Indian Institute of Technology, Indore

Dedicated to My Parents
and
My Sister

Abstract

The research presented investigates the electrochromic properties of various materials, including metal oxides and conducting polymers, for potential applications in smart optoelectronic devices. Methods such as sol-gel synthesis, drop casting, and co-precipitation were employed to synthesize these materials, followed by characterization using techniques like cyclic voltammetry, electrochemical impedance spectroscopy, UV-Vis spectroscopy, scanning electron microscopy, X-Ray diffraction and Raman spectroscopy. The study compares the performance of different doping materials in terms of color switching time, stability, color contrast, coloration efficiency and reversibility at two different wavelengths. Results show promising outcomes, particularly with zinc oxide and tungsten trioxide doping, demonstrating enhanced coloration efficiency and stability. Moreover, the investigation suggests avenues for further research, such as exploring alternative synthesis methods to optimize material properties for specific device applications. Overall, the study contributes to advancing the understanding and development of electrochromic device for diverse optoelectronic technologies.

TABLE OF CONTENTS

LIST OF FIGURES

LIST OF TABLES

NOMENCLATURE

E	Energy
λ	Wavelength
υ	Frequency
h	Planck's constant
c	Speed of light
T	Transmittance
A	Absorbance

ACRONYMS

EM	Electromagnetic
UV	Ultraviolet
UV-Vis	Ultraviolet-Visible
HOMO	Highest Occupied Molecular Orbital
LUMO	Lowest Unoccupied Molecular Orbital
i.e.	That is
CV	Cyclic Voltammetry
WE	Working Electrode
CE	Counter Electrode
RE	Reference Electrode
V	Volts

Chapter 1

INTRODUCTION

1.1 Electrochromism

Electrochromism, a captivating phenomenon in materials science, refers to the ability of certain substances to undergo visible changes in optical properties when subjected to an electrical stimulus[1]. These materials, termed electrochromic materials (ECMs), hold immense promise for a range of applications due to their dynamic color-switching capabilities. The field of electrochromism has witnessed significant advancements since its inception in the early 1960s, with researchers continuously exploring novel materials, device architectures, and performance optimization strategies.

Fundamentally, electrochromic behavior arises from redox reactions occurring at the interface between electrodes and electrolytes, leading to alterations in the material's absorption or transmission properties across the electromagnetic spectrum. By modulating the electrical bias applied to electrochromic devices (ECDs), reversible changes in color or opacity can be achieved, offering opportunities for applications in smart windows, displays, eyewear, and adaptive camouflage systems. Understanding the underlying mechanisms of electrochromism and refining ECM properties are essential steps towards unlocking their full potential in diverse technological domains.

1.2 Motivation

Working in electrochromic devices (ECDs) presents an exciting opportunity to delve into a dynamic field with wide-ranging applications. Studying electrochromism allows us to understand the fundamental processes behind color changes in response to electrical stimuli, paving the way for the development of advanced materials and devices. By optimizing the performance of ECDs, we can enhance their energy efficiency, durability, and functionality, leading to innovations in smart windows, displays, and energy-saving technologies. The interdisciplinary nature of electrochromism research fosters collaboration between scientists and engineers from various disciplines, driving innovation and solutions to pressing societal and environmental challenges. Ultimately, working in electrochromic devices offers a

rewarding path towards developing transformative technologies with tangible benefits for society, industry, and the environment.

1.3 Types of electrochromic materials

Electrochromic materials (ECMs) encompass a diverse array of substances that exhibit bias-induced color switching, making them integral to electrochromic devices. Broadly categorized into organic and inorganic types[1], ECMs offer varying properties and functionalities tailored to specific applications. Inorganic ECMs primarily comprise transition metal oxides (TMOs) such as tungsten, vanadium, chromium, cobalt, iron, manganese, molybdenum, nickel, niobium, palladium, and titanium oxides. Additionally, conducting polymers (CPs) like polyaniline (PANI), polythiophene (P3HT), PEDOT: PSS, polypyrrole (PPy), and polyindole (PI) exhibit electrochromic behavior owing to their multiple redox states. Viologens, including bipyridine derivatives, exist as molecular and polymeric forms, exhibiting significant electrochromic activity. Another notable class comprises hexacyanometalletes like Prussian Blue (PB), offering multiple-colored states. Metallopolymers, featuring metal-to-ligand charge transfer, demonstrate long-term stability and efficient switching times. Recent advancements have introduced novel ECMs such as microporous metal/covalent organic frameworks (MOFs/COFs), organic-halide hybrid perovskites, MXenes, and composite structures, expanding the library of ECMs with diverse colors, origins, and functionalities, thus paving the way for innovative electrochromic applications.

1.4 Electrochromic Device

Fabricating an electrochromic device (ECD) involves several steps to assemble its five-layered structure. Initially, two transparent conducting substrates, typically made of Indium/Fluorine Tin Oxide (ITO/FTO) coated glasses[2,3], are prepared as outer layers for applying bias. Chromophores are then deposited onto one or both of these substrates using techniques such as spin coating, spray casting, hydrothermal, or electrodeposition, forming thin films known as EC electrodes. The second substrate is loaded with an ion-storage layer, and the two electrodes are integrated together with a gel electrolyte in between. Employing the flip-chip method, the sturdy ECD is obtained with its ends ready to be connected to a power supply (Figure 1.1). The gel electrolyte, containing highly mobile ions, facilitates electron movement, resulting in color changes around the active electrode. The type of ECD fabricated—transmissive or reflective—depends on the choice of electrochromic materials (ECMs) and the substrate used. For flexibility or stretchability, glass substrates are often replaced with electrodes like polyethylene

terephthalate (PET). While the standard five-layered structure is common, deviations exist based on specific requirements and applications, including variations in the number of layers or types of substrates used. Additionally, measurements are conducted on EC electrodes to understand their properties, followed by fabrication of Monolayer and bi-layer ECDs before exploring all-in-one EC gel configurations.

Figure 1.1: Basic schematic of an electrochromic device

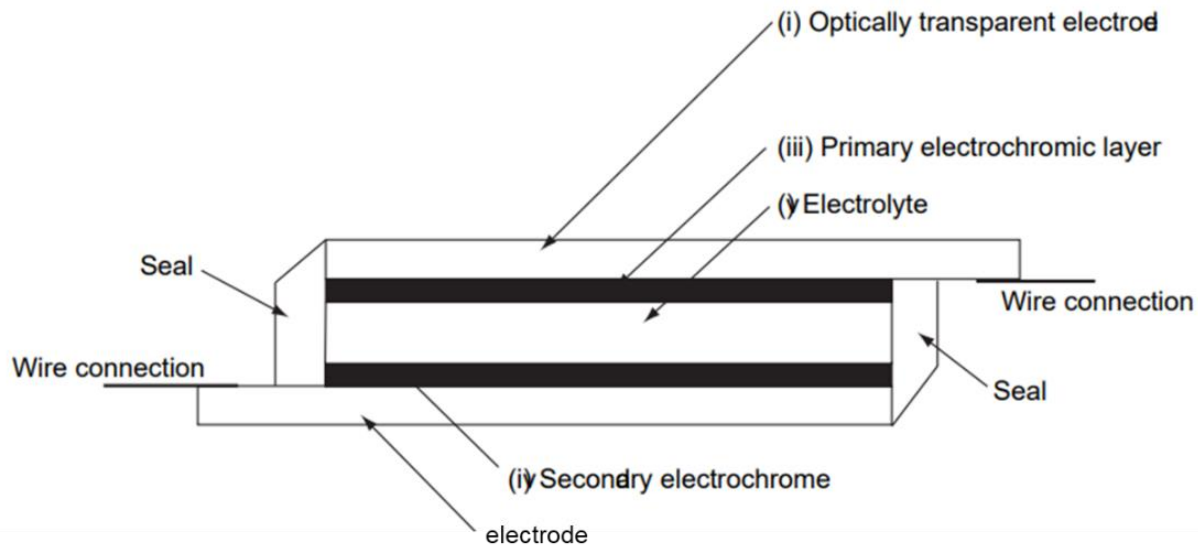

Device durability is defined by five criteria[4]:

1. The environment for a specific application, which dictates the required operational speed.
2. The upper and lower temperatures of operation (considering variations worldwide).
3. Stresses induced by thermal shock during rapid cooling and warming.
4. Deterioration due to solar exposure, particularly by UV light.
5. Additional stresses like changes in humidity and mechanical shock. Devices relying on proton movement may need water, and the concentration of water should remain within a narrow, desirable range. Sealing is crucial to maintain internal humidity levels, protect against oxygen ingress, and ensure device robustness.

1.5 Device performance parameters

Once the device is fabricated, we need to thoroughly access it performance on various parameters as mentioned below.

1.5.1 Switching time

Applying a voltage triggers the electrochromic device [1](ECD) to transition between optical states, known as coloration and bleaching, in a reversible manner. The time taken for this transition, termed as the switching time, is defined as the duration required for a 90% (Note:

in some papers researchers take 67 % change in absorbance values as the threshold) change in absorbance during both coloration (T_c) and bleaching (T_b) processes. While T_c and T_b are typically similar in magnitude, they may not be identical due to the distinct microscopic processes governing coloration and bleaching.

1.5.2 Cyclic stability

To assess the cyclic stability of electrochromic [1]devices (ECDs), researchers evaluate their cycle life by subjecting them to continuous voltage pulses of specific durations. The optical output response is then recorded to observe any variations in the contrast value over multiple coloration/bleaching cycles. An ECD demonstrating minimal changes in colored states even after numerous cycles is indicative of good cyclic stability, highlighting its suitability for prolonged usage and practical applications.

1.5.3 Color contrast

The visibility and distinguishability [1]of different states in an electrochromic device (ECD) are crucial. The color contrast, representing the maximum difference in absorbance values between the device's colored and bleached states, is quantified using the equation:

$$\boldsymbol{C.C = \frac{|T_f - T_i|}{T_f} \times 100} \quad \textbf{or} \quad \boldsymbol{C.C = \frac{|A_f - A_i|}{A_f} \times 100} \tag{1.1}$$

Here, A_f / T_f and A_i / T_i represent the final and initial absorbance/Transmittance values at a specific wavelength, respectively. The resulting color contrast value is expressed as a percentage, providing a quantitative measure of the device's optical performance and distinguishability between its various states.

1.5.4 Coloration efficiency (CE)

The charge efficiency (CE) value, [1]denoted as 'η' and expressed in units of cm^2/C, serves as a key parameter indicating the power efficiency of an electrochromic device (ECD). It quantifies the amount of charge required for inducing a change in optical density or contrast, represented by ΔOD. The CE value is calculated using the formula:

$$\boldsymbol{\eta = \Delta OD / Q} \tag{1.2}$$

Here, ΔOD signifies the difference between the maximum and minimum absorbance values, while Q represents the charge intercalated or deintercalated by the device to achieve the observed change in optical density. The physical value of CE is determined from the slope of

a curve plotting the variation of optical density (OD) against charge (Q), providing valuable insights into the device's power efficiency and performance characteristics.

1.6 Multifunctional applications

Electrochromic devices (ECDs) have revolutionized various industries, serving as smart switchable windows, rear-view mirrors, curtains, and displays. Despite their widespread adoption, challenges such as cost, efficiency, and durability persist. To address these issues, researchers are developing electrodes and devices[3]capable of multifunctionality, including charge storage, sensing, memory, and catalysis. Certain electrochromic materials exhibit excellent charge storage capacities, making them ideal for electrochemical supercapacitors with superior energy densities and lower input requirements. Additionally, some materials possess electrocatalytic properties crucial for sustainable applications like water splitting for hydrogen production. These advancements represent a significant milestone in material science, paving the way for multifunctional devices with enhanced performance. Furthermore, in my work the ECD's high absorbance in the infrared (IR) region enables it to function as a heat-blocking window, effectively mitigating solar heat gain and keeping the building cool passively without the need for air conditioning. By reducing the reliance on artificial cooling systems, the ECD contributes to energy savings and promotes sustainability in building design. This dual functionality of color switching and heat blocking makes the ECD an attractive solution for enhancing comfort and energy efficiency in architectural applications.

Chapter 2

EXPERIMENTAL TECHNIQUES

All chemicals utilized in this investigation, including ethyl viologen diperchlorate, poly(3-hexyl thiophene-2,5 diyl), sodium tungstate dihydrate ($Na_2WO_4.2H_2O$), Zinc nitrate hexa-hydrate ($Zn(NO_3)_2.6H_2O$), Sodium Hydroxide (NaOH), Hydrochloric acid (HCl), Titanium n-butoxide, Sodium molybdate dihydrate ($Na_2Mo_4.2H_2O$), Citric acid ($C_6H_8O_7$), lithium perchlorate ($LiClO_4$), polyethylene oxide (PEO), nitric acid (HNO_3, 38%), and sulfuric acid (H_2SO_4, 98%), were procured from Alfa Aesar. Analytical grade reagents, such as acetone, 1,2-dichlorobenzene (DCB, anhydrous), acetonitrile (ACN, anhydrous, 99%), ethanol, methanol, and isopropyl alcohol (IPA), were sourced from Sigma AldrichTM and used as received. Substrates, namely Indium Tin Oxide (ITO) and Fluorine doped Tin Oxide (FTO) coated glasses were obtained from Macwin India and were sliced into pieces measuring 2x1 cm^2. The selection of ITOs and FTOs as the substrate of interest was motivated by their high conductivity and transparency, essential requirements for electrochromic (EC) devices

2.1 Electrode fabrication techniques

These ITOs and FTOs substrates were then transformed into electrodes by depositing the desired EC material onto them using one of the below-mentioned techniques, all of which are bottom-up approaches.

2.1.1 Spin coating method

Spin coating, hailed as one of the simplest techniques for depositing samples onto flat surfaces, guarantees the uniformity of thin films across the substrate area. This method relies on centrifugal force to spread the material evenly over the substrate, ensuring complete coverage. The procedure involves several steps: firstly, the substrate is securely placed onto the sample holder within the spin coater machine and affixed using a vacuum pump. Then, a specified volume of solution, typically ranging from 10 to 50 µl, is applied to the substrate. Subsequently, the deposition occurs at a consistent spin rate for a predetermined duration to achieve the desired thin film (Figure 2.1). Following deposition, the films undergo drying at temperatures between 80º and 100º C to eliminate excess solvent. Spin coating offers numerous advantages, including its straightforward fabrication process, uniform coating distribution, and precise

control over film thickness, making it particularly suitable for coating organic materials and polymers.

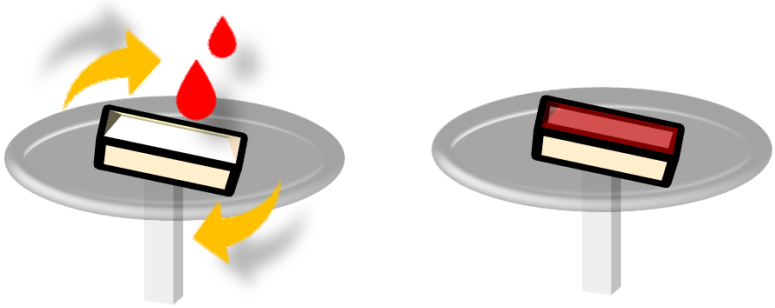

Figure 2.1: Schematic showing the spin coating mechanism.

(Image credit: PhD thesis of Dr. Tanushree Ghosh)

2.1.2 Drop Casting

Drop casting deposits a solution onto a substrate, evaporating the solvent to form thin films. Versatile and cost-effective, it's ideal for lab-scale research and large-scale production. Film thickness is controlled by solution concentration, droplet volume, and substrate properties. Suitable for various applications including electronics and biomedical devices.

2.2 Synthesis methods for dopant materials

2.2.1 Hydrothermal method

The conventional method, known as hydrothermal deposition, utilizes elevated temperatures and water as its primary components for film deposition, as indicated by its name. The procedure involves several steps: firstly, a precursor solution is prepared by mixing the necessary chemicals with an appropriate amount of deionized (DI) water, which is continuously stirred. Next, this solution is transferred into a teflon-coated autoclave, where the substrate is positioned. Subsequently, the entire autoclave containing the solution is sealed within a stainless container to prevent air exchange. The setup is then placed into a furnace, where high temperatures are applied for an extended period, facilitating film deposition (Figure 2.2). The fundamental principle revolves around vaporizing the water component of the precursor solution and depositing the remaining material onto the substrate. This method offers the advantage of enabling the growth of large crystals while maintaining the desired film composition.

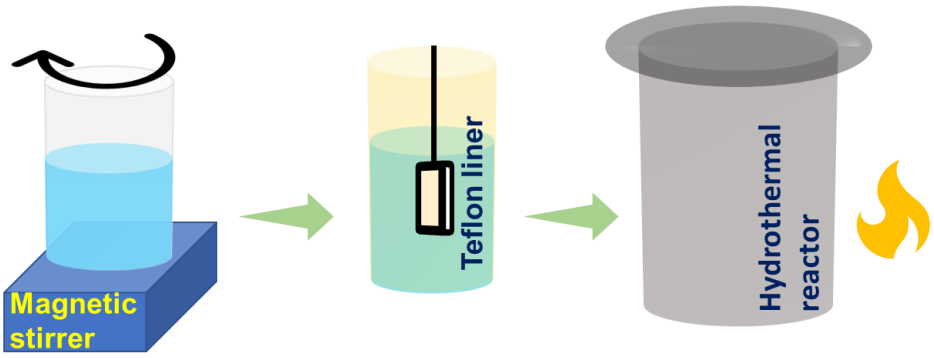

Figure 2.2: Schematic showing various parts of hydrothermal method.(Image credit: PhD thesis of Dr. Tanushree Ghosh)

2.2.2 Co-precipitation method

The co-precipitation method is a widely used technique for synthesizing nanoparticles and composite materials. In this method, two or more precursor compounds are dissolved in a solvent, typically water, to form a homogeneous solution. Subsequently, a precipitating agent, such as a base or acid, is added to the solution under controlled conditions, leading to the simultaneous precipitation of multiple compounds or elements. The reaction conditions, including temperature, pH, and stirring rate, play crucial roles in determining the size, morphology, and composition of the precipitated particles. After precipitation, the resulting solid is typically collected by filtration, washed to remove impurities, and dried. The co-precipitation method offers several advantages, including simplicity, scalability, and the ability to control the composition and properties of the resulting materials by adjusting reaction parameters. This versatile technique finds applications in various fields, including materials science, catalysis, environmental remediation, and biomedical research, where the synthesis of tailored nanoparticles and composite materials is desired.

2.2.3 Sol-gel method

The sol-gel method synthesizes materials by converting a sol (a colloidal suspension) into a gel and then solidifying it. It involves hydrolysis and condensation reactions of metal alkoxides in a liquid solution, typically alcohol. This process forms a network of interconnected nanoparticles. By controlling parameters like temperature and pH, the resulting material's structure and properties can be tailored. Sol-gel is versatile, producing thin films, fibers, and bulk materials. Widely used in ceramics, glasses, and coatings, it offers advantages such as low

processing temperatures and homogeneity. Its applications range from optics and electronics to biomedicine and catalysis.

2.3 Characterization techniques

Upon synthesizing materials, it's imperative to conduct characterization to ascertain their composition and properties accurately.

2.3.1 Scanning Electron Microscopy (SEM)

Scanning Electron Microscopy (SEM) is a powerful imaging technique used to visualize the surface morphology, composition, and topography of materials at high resolution. It employs a focused beam of electrons to probe the surface of a sample, generating detailed images with magnifications ranging from tens to hundreds of thousands of times.

Instrumentation:

1. Electron Source: SEMs utilize an electron gun to produce a beam of electrons. The electron source typically consists of a tungsten filament or a field emission gun (FEG) capable of emitting electrons with high energy and brightness.

2. Electron Optics: The electron beam is focused and directed onto the sample surface by a series of electromagnetic lenses and apertures. The optics system controls the size, shape, and intensity of the electron beam, enabling precise imaging and analysis of the sample.

3. Sample Stage: The sample is mounted on a stage that allows for precise positioning and manipulation during imaging. The stage may provide options for tilt, rotation, and XYZ movement to facilitate imaging from different perspectives and angles.

4. Detectors: SEMs are equipped with various detectors to capture different signals emitted or generated by the sample in response to the electron beam. Common detectors include secondary electron detectors (SE), backscattered electron detectors (BSE), and energy-dispersive X-ray spectrometers (EDS).

5. Imaging System: The signals detected by the detectors are converted into visual images displayed on a monitor or computer screen. SEM images can be acquired in real-time or saved for further analysis and processing.

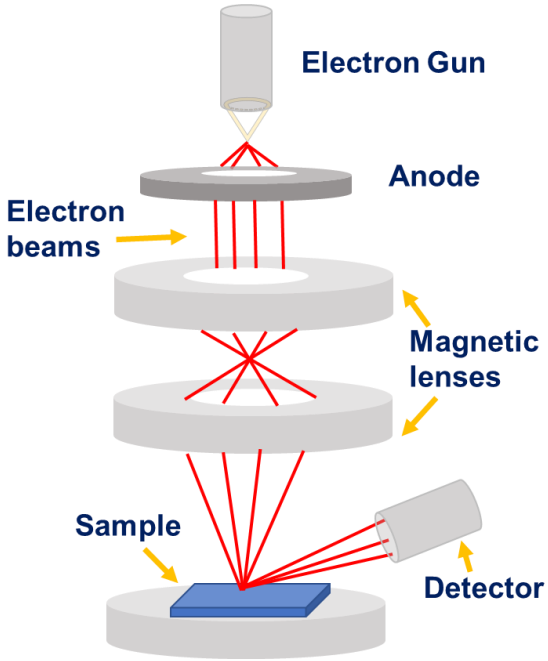

Figure 2.3: Schematic showing various parts of an electron microscope

(Image credit: PhD thesis of Dr. Tanushree Ghosh)

Operation:

1. Electron Beam: The electron beam is generated by the electron source and focused onto the sample surface. The beam interacts with the atoms in the sample, causing various electron emissions and signals to be produced.

2. Signal Detection: Depending on the interaction of the electron beam with the sample, different signals are emitted or generated, including secondary electrons (SE), backscattered electrons (BSE), and characteristic X-rays. These signals are detected by the corresponding detectors.

3. Image Formation: The detected signals are processed and converted into visual images displayed on a monitor. SEM images reveal detailed surface features, topography, and composition of the sample with high resolution and magnification.

4. Analysis: SEM images can be analyzed to extract quantitative information about the sample, including particle size and distribution, surface roughness, elemental composition, and phase identification. Additional techniques such as EDS can be used for elemental analysis and mapping.

Applications:

SEM finds wide-ranging applications in materials science, nanotechnology, biology, geology, forensics, and semiconductor industry. It is used for surface characterization, defect analysis, failure analysis, quality control, and research in diverse fields. SEMs are indispensable tools for studying microstructures, nanoparticles, biological specimens, and engineered materials, providing valuable insights into their properties, behavior, and performance.

2.3.2 Raman Spectroscopy

Raman spectroscopy is a powerful analytical technique used to provide detailed information about the vibrational and rotational modes of molecules. It offers insights into molecular structure, composition, and interactions by measuring the inelastic scattering of light, known as Raman scattering, caused by the interaction of photons with chemical bonds within a sample.

Instrumentation:

1. Laser Source: A monochromatic laser source is used to illuminate the sample. Common lasers employed in Raman spectroscopy include visible (such as green or red) and near-infrared lasers. The choice of laser depends on factors such as the sample's optical properties and the desired spectral range.

2. Optics: The laser beam is directed onto the sample through a series of lenses, mirrors, and filters. Optics are used to focus the laser beam onto the sample, collect the scattered light, and direct it to the detector.

3. Sample Chamber: The sample is typically placed in a sample chamber, which may be equipped with temperature control and environmental control capabilities to optimize measurements under specific conditions.

4. Detector: A sensitive detector, such as a charge-coupled device (CCD) or photomultiplier tube (PMT), is used to measure the intensity of the Raman scattered light. The detector converts the optical signal into an electronic signal that can be processed and analyzed.

5. Spectrometer: A spectrometer is used to disperse the Raman scattered light into its component wavelengths. It consists of diffraction gratings or prisms and allows for the selection of specific spectral regions for analysis.

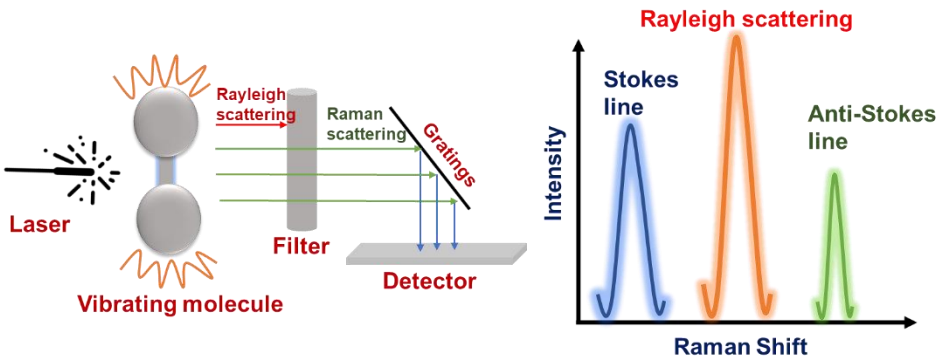

Figure 2.4: Schematic showing basic mechanism of Raman spectroscopy.
(Image credit: PhD thesis of Dr. Tanushree Ghosh)

Operation:

1. Excitation: The laser beam is focused onto the sample, leading to the excitation of molecular vibrations. A small fraction of the incident photons undergoes inelastic scattering, resulting in Raman scattering.

2. Scattering: The scattered light contains both Rayleigh scattering, which has the same frequency as the incident laser light, and Raman scattering, which has shifted frequencies corresponding to the vibrational modes of the molecules in the sample.

3. Detection: The Raman scattered light is collected by the optics and directed to the detector. The detector measures the intensity of the scattered light as a function of its wavelength.

4. Analysis: The Raman spectrum, which represents the intensity of scattered light as a function of Raman shift (frequency difference from the incident laser), is analyzed to extract information about molecular vibrations, chemical bonds, and structural properties of the sample.

Applications:

Raman spectroscopy finds applications in various fields, including chemistry, materials science, pharmaceuticals, biology, and forensics. It is used for qualitative and quantitative analysis of chemical compositions, identification of unknown substances, characterization of molecular structures, monitoring of chemical reactions, and investigation of biological specimens. Additionally, Raman spectroscopy can be performed in situ, in real-time, and non-destructively, making it a valuable tool for research, quality control, and process monitoring in diverse industries.

Spectroscopy involves examining how light interacts with matter. Light, as a form of energy within the electromagnetic spectrum, engages in quantum phenomena when interacting with matter. These interactions depend on both the properties of the electromagnetic radiation and the characteristics of the samples under study. The electromagnetic radiation spectrum, displaying increasing wavelength and decreasing energy, is illustrated in a figure 2.1 from left to right.

2.3.3 X-Ray Diffraction (XRD)

X-ray diffraction (XRD) is a powerful analytical technique used to analyze the crystal structure, phase composition, and atomic arrangement of materials. It is based on the principle of elastic scattering of X-rays by atoms in a crystal lattice, resulting in the generation of diffraction patterns that provide valuable information about the structure and properties of the material.

Instrumentation:

1. X-ray Source: X-ray diffraction requires a source of monochromatic X-rays, typically generated by an X-ray tube operating at high voltage. The X-ray source emits a narrow beam of X-rays with a specific wavelength, typically in the range of 0.1 to 2.5 angstroms.

2. Sample Holder: The sample is mounted on a sample holder, which positions it in the path of the X-ray beam. The sample holder may allow for precise orientation and rotation of the sample to obtain diffraction patterns from different crystallographic planes.

3. Detector: A detector is used to measure the intensity of the diffracted X-rays as a function of the diffraction angle (2θ). Common detectors include scintillation detectors, semiconductor detectors, and imaging plates. Modern XRD instruments often utilize electronic detectors for high sensitivity and rapid data acquisition.

4. Goniometer: A goniometer is used to position the sample holder and detector relative to each other, allowing for precise control of the diffraction geometry. The goniometer can rotate the sample around multiple axes to collect diffraction data from different orientations.

5. Data Acquisition System: A data acquisition system is used to record and process the diffraction data collected by the detector. This system may include software for controlling instrument parameters, collecting diffraction patterns, and analyzing the resulting data.

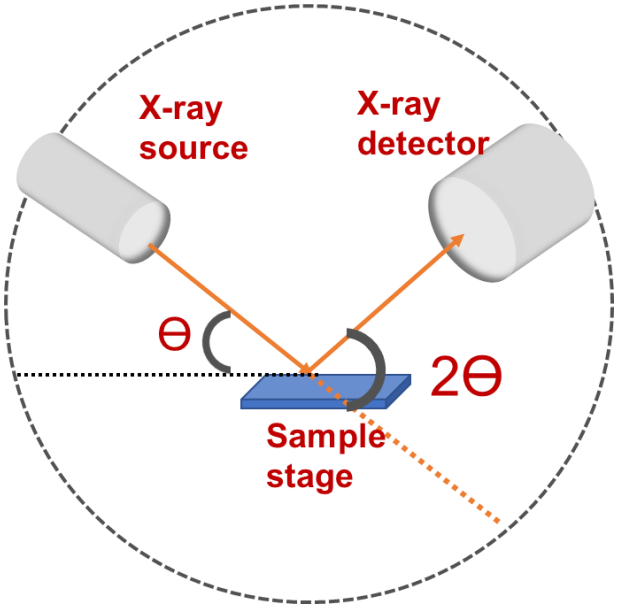

Figure 2.5: Schematic of an X-ray diffractometer.

(Image credit: PhD thesis of Dr. Tanushree Ghosh)

Operation:

1. Incident X-rays: The X-ray beam emitted by the X-ray source is directed onto the sample at a specific angle of incidence. The X-rays interact with the atoms in the crystal lattice of the sample, causing them to scatter in different directions.

2. Diffraction: The scattered X-rays interfere constructively or destructively, depending on the spacing between the atomic planes in the crystal lattice. This results in the generation of a diffraction pattern consisting of discrete peaks corresponding to the diffraction angles (2θ) at which constructive interference occurs.

3. Data Collection: The diffracted X-rays are collected by the detector and converted into electrical signals. The intensity of the diffracted X-rays is recorded as a function of the diffraction angle (2θ) to generate a diffraction pattern.

4. Analysis: The diffraction pattern is analyzed to extract information about the crystal structure, phase composition, and orientation of the sample. This may involve comparing the experimental diffraction pattern with reference patterns from known crystal structures, performing quantitative phase analysis, and determining lattice parameters and crystallographic orientation.

Applications:

X-ray diffraction is widely used in various fields, including materials science, chemistry, geology, and biology. It is employed for phase identification, crystallographic analysis, texture measurement, residual stress analysis, and defect characterization in a wide range of materials, including metals, ceramics, polymers, minerals, and pharmaceuticals. XRD is indispensable for research, quality control, and process optimization in industries such as manufacturing, aerospace, automotive, electronics, and pharmaceuticals.

2.3.4 UV-Vis spectroscopy

The machine used to perform the experiment is PerkinElmer UV/VIS Lambda 365.

Figure: 2.6: UV-Vis Spectroscopy.

UV-Vis spectroscopy, short for ultraviolet-visible spectroscopy, is a technique used to analyze the absorption and transmission of light by a substance across the UV and visible regions of the electromagnetic spectrum. This method provides valuable insights into a material's electronic structure, concentration, and chemical environment. UV-Vis spectroscopy involves passing light through a sample and measuring the absorbance or transmittance at various wavelengths. The instrumentation typically consists of a UV-Vis spectrophotometer equipped with a light source, monochromator, sample holder, and detector (Figure 2.7). By comparing the absorbance spectrum of a sample to reference spectra, researchers can identify compounds and quantify their concentration. UV-Vis spectroscopy finds applications in various fields, including chemistry, biochemistry, environmental science, and pharmaceuticals, for analyzing compounds such as organic molecules, metal ions, and biological macromolecules.

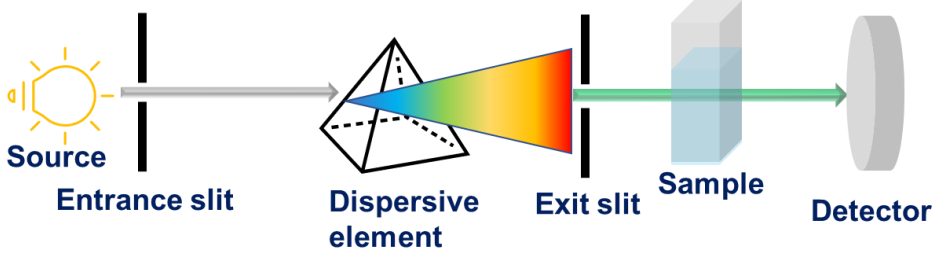

Figure 2.7: Schematic of an UV-Vis spectrometer

(Image credit: PhD thesis of Dr. Tanushree Ghosh)

2.3.5 Electrochemistry

Electrochemistry investigates chemical properties influenced by applied current or bias, crucial for understanding redox behavior and electron/mass transport phenomena. Electrochemical studies employ a three-electrode cell setup alongside an electrolytic solution. Experimental setups utilized instruments such as the Keithley-2450 source meter and the Metrohm Autolab Potentiostat for data acquisition. These tools enable precise control over current and voltage conditions, facilitating the characterization of sample properties. Through electrochemical analysis, researchers gain insights into reaction mechanisms, kinetics, and interfacial processes, contributing to the comprehensive understanding of material behavior and facilitating advancements in various fields, including energy storage, corrosion prevention, and sensor development.

Figure 2.8: Autolab PGSTAT101

(Image credit: Google)

2.3.5.1 Cyclic Voltammetry (CV)

Cyclic voltammetry is a powerful electrochemical technique used to investigate the redox properties of materials. It involves sweeping the potential of a working electrode linearly over time while measuring the resulting current. The cyclic voltammogram obtained provides information about the electrochemical behavior of the system, including oxidation and reduction potentials, electron transfer kinetics, and diffusion coefficients. This technique is widely used in various fields, including battery research, corrosion studies, and sensor development, due to its simplicity, versatility, and ability to provide valuable insights into the electrochemical processes occurring at the electrode-electrolyte interface. Experimental setups typically involve a three-electrode cell configuration with a working electrode, reference electrode, and counter electrode, controlled by a potentiostat.

2.3.5.2 Electrochemical Impedance Spectroscopy (EIS)

Electrochemical impedance spectroscopy (EIS) is a powerful technique used to study the electrical properties of electrochemical systems. It involves applying a small amplitude sinusoidal potential or current to a system over a range of frequencies and measuring the resulting impedance. EIS provides valuable information about the resistive and capacitive components of the system, as well as its frequency-dependent behavior. This technique is widely used to study phenomena such as charge transfer processes, diffusion, adsorption, and corrosion kinetics. EIS is particularly valuable for characterizing the performance of batteries, fuel cells, sensors, and corrosion protection coatings. Experimental setups typically involve a potentiostat or impedance analyzer coupled with a three-electrode cell configuration, allowing precise control over the applied signals and measurement of the system's response.

2.4 Synthesis of Zinc Oxide (ZnO)

The ZnO nanoparticles were synthesized using co-precipitation method. The typical [5]synthesis is as follows: the alkali solution of zinc was prepared by dissolving zinc nitrate hexahydrate [$Zn(NO_3)_2 \cdot 6H_2O$] in 50 ml deionized water and NaOH in another 50 ml deionized water in the molar ratio [Zn^{2+} = 1M, OH^- = 2M]. Then the NaOH solution was kept at 35℃. Under constant stirring, the zinc nitrate solution was added slowly (dropwise for 30 min) to the above alkali solution. After a 3 hours reaction under constant stirring, the solution is allowed to settle. A white precipitate was deposited in the bottom of the flask and was collected using filter paper and washed several times with absolute ethanol and distilled water to remove any unreacted chemicals and $NaNO_3$. The precipitate mostly consists of $Zn(OH)_2$ and ZnO. Finally, the ZnO powder is obtained by dehydration of $Zn(OH)_2$ at 130°C for 9 hours in an oven[6].

$$Zn(NO_3)_2 + 2\,NaOH \rightarrow 2\,Zn(OH)_2 + 2\,NaNO_3 \quad (2.1)$$

$$2\,Zn(OH)_2 \rightarrow 2\,ZnO + 2\,H_2O \quad \text{(at 130°C for 9 h)} \quad (2.2)$$

To increase the precipitate formation and maximizing the yield we tried not to use excess NaOH as the precipitate of zinc hydroxide will dissolve, forming a colourless solution of zincate ion. We can also keep the temperature low after mixing the zinc nitrate solution with the sodium hydroxide solution. This will reduce the solubility constant of zinc hydroxide and it will precipitate out of the solution.

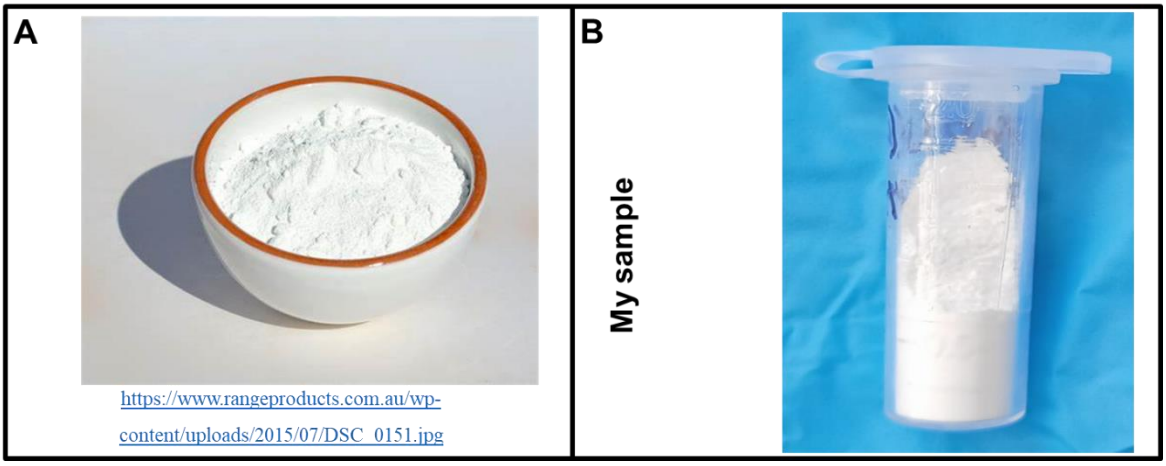

Figure 2.9: ZnO sample

2.5 Synthesis of Tungsten trioxide (WO_3)

To produce ultrafine WO_3 powder, a straightforward [7]co-precipitation technique was employed. Initially, 0.33 g of Sodium tungstate was dissolved in 20 ml of distilled water and stirred continuously. Subsequently, 2 M HCl was gradually added to the solution to maintain a pH of 1.5, followed by stirring for 13 hours. The resulting precursor solution was then washed thrice with deionized water and ethanol to eliminate impurities. The precipitate obtained was dried for 16 hours at 50 °C, yielding greenish-blue powder. This powder underwent calcination at 450 °C for 24 hours. Following calcination, the powder was stored in a desiccator for further characterization without additional purification.

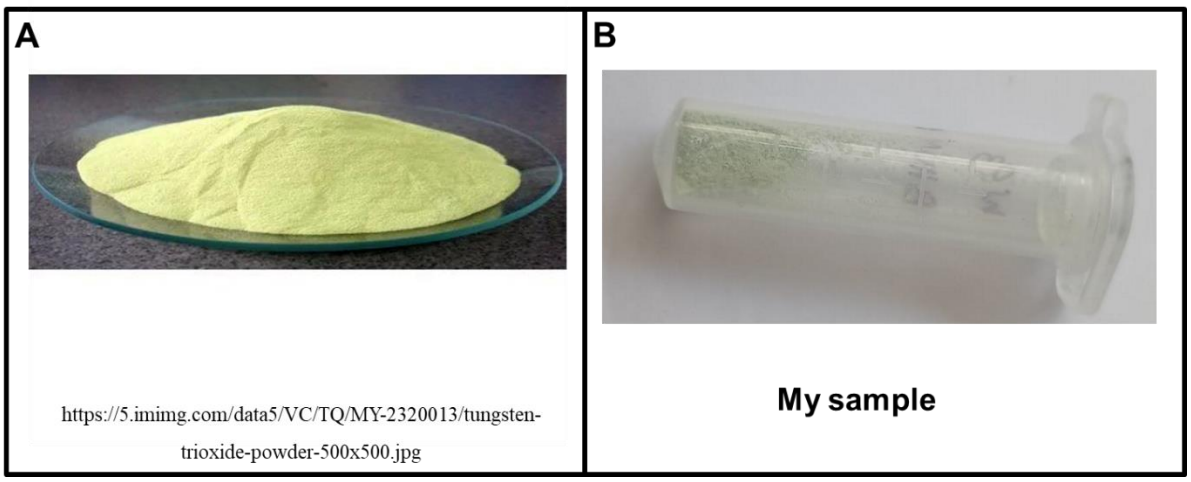

Figure 2.10: WO_3 sample

2.6 Synthesis of Titanium dioxide (TiO_2)

TiO_2 is synthesized using hydrothermal method. The typical synthesis is as follows, combine 15 mL of HCl with 15 mL of distilled water and stir for 10 minutes[8]. Next, add 400 µL of titanium n-butoxide to the solution and continue stirring for another 10-12 minutes. Transfer the mixture into an autoclave and heat it at 150 °C for 9 hours. Then, filter the mixture using filter paper and wash the residue several times with distilled water. Allow the powder to dry in an oven for 3 hours at 80 °C.

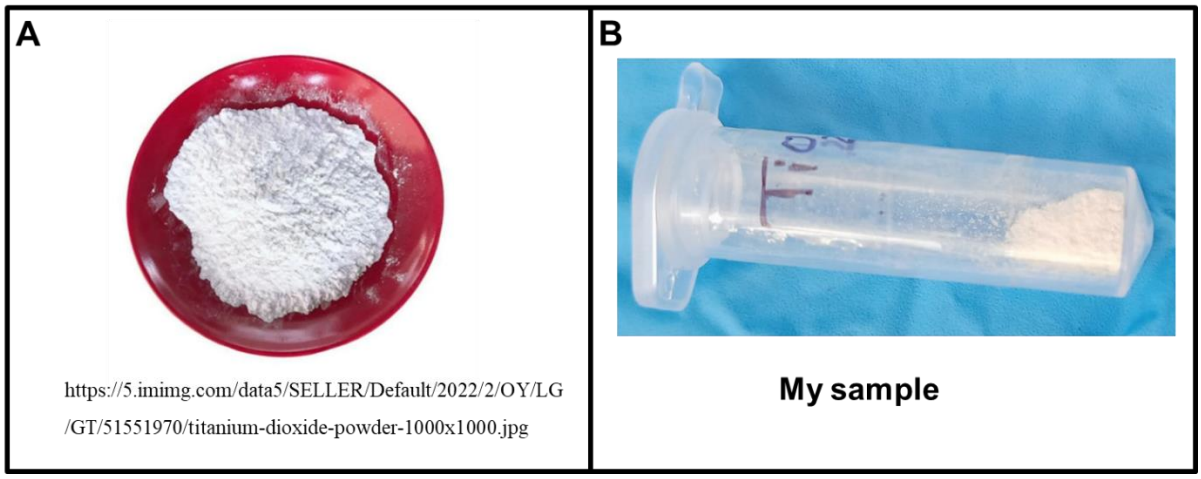

Figure 2.11: TiO_2 sample

2.7 Synthesis of Molybdenum trioxide (MoO_3)

Sodium molybdate dihydrate ($Na_2Mo_4.2H_2O$), citric acid ($C_6H_8O_7$), and nitric acid (HNO_3) were utilized in the synthesis of molybdenum trioxide [9]powder via the sol-gel method. The precursor solution was formulated by dissolving 0.01 M (50 mg) sodium molybdate in 20 mL of deionized water. Subsequently, 0.016 M of HNO_3 (20 µL) was added dropwise to the precursor solution with continuous stirring for over 30 minutes. To act as a surfactant, 0.1 M citric acid was incorporated into the solution and stirred for 1 hour. The resultant solution was then subjected to heating in an oven at 120°C for 6 hours. Following this, the resulting precipitate was annealed at 450°C for 3 hours under an inert atmosphere. The powder obtained after annealing was collected for further characterization without undergoing any purification steps.

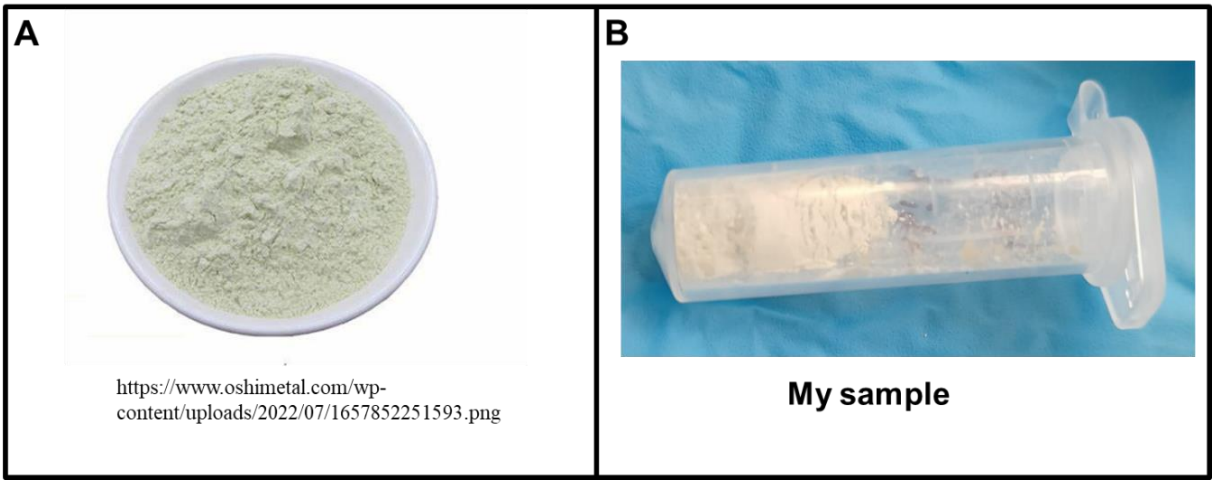

Figure 2.12: MoO_3 sample

2.8 Device Fabrication

2.8.1 Preparation of P3HT electrode: For fabrication of electrochromic device, 0.3 wt% P3HT solution in DCB (1, 2- Dichlorobenzene) was prepared by vortex mixing. . The P3HT film was spin-coated on ITO-coated glass substrate (commercially procured) at 600 rpm for 120s and annealed at 80 ◦C for 1 h.

2.8.2 Preparation of Gel Electrotyte: 5 wt% of PEO is mixed with ACN and mixed thoroughly to form gel-like substance.

2.8.3: Preparation of EV electrode: 4 wt% Ethyl Viologen diperchlorate is mixed with ACN.

2.8.4: Device assembly: We then take the required metal oxide ($ZnO/WO_3/TiO_2/MoO_3$ as per need) as our dopant and mix it with EV in the proportion 0.1 wt%. We then mix the solution with PEO in equal proportion. The combined mixture is drop casted onto an ITO coated glass

substrates and then assemble together with the help of double-sided tape to keep the both ITO substrates attached with each other.

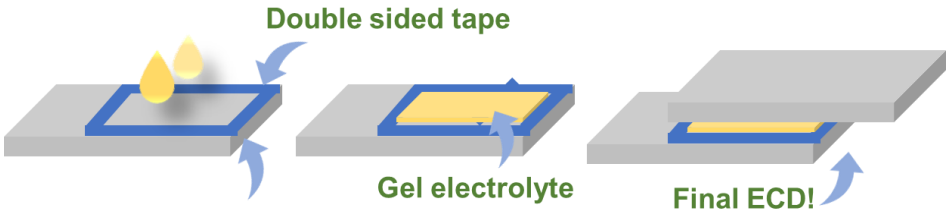

Figure 2.13: Schematic showing step by step method of device fabrication

(Image credit: PhD thesis of Dr. Tanushree Ghosh)

2.9 Ethyl Viologen diperchlorate (EV)

Ethyl viologen diperchlorate (EV) is a chemical compound commonly used in various electrochemical applications. It consists of a viologen moiety with two ethyl groups attached to the nitrogen atoms and perchlorate ions as counterions[10]. EV is known for its reversible redox properties, making it suitable for use as an electron shuttle or mediator in redox reactions. Its ability to undergo rapid and reversible reduction-oxidation processes makes it valuable in systems such as batteries, sensors, and electrochromic devices[11]. Additionally, EV's stability and solubility in polar solvents contribute to its versatility in electrochemical studies and applications.

How Viologens show color: Viologens, more formally known as 1,1′-disubstituted-4,4′-bipyridilium salts, are recognized as electrochromic materials exhibiting a diverse range of colors dependent on their radical substituents. These compounds undergo sequential electron-transfer reactions, progressing from the di-cationic state to a radical cation, and finally forming a neutral species[12]. Each step in this process yields distinct colors determined by the specific substituents present. The term "viologen" originates from the violet hue produced when 1,1′-dimethyl-4,4′-bipyridilium is reduced by a single electron, resulting in the formation of the radical cation[13]. The di-cationic form stands as the most stable among the three common viologen redox states, appearing colorless in its pure form, unless optical charge transfer with the counter anion occurs. The radical cation, known for its vibrant coloration, arises from intense intramolecular optical charge transfer. Radical cations with short alkyl chains exhibit a blue (or blue-purple in concentrated solutions) color, transitioning to crimson as the alkyl chain length increases due to enhanced dimerization. Conversely, the neutral species typically appear

uncolored. Thus the electrochromic mechanism involves reversible redox reactions of ethyl viologen molecules, manifesting in three possible states: di-cation, radical cation, and neutral.

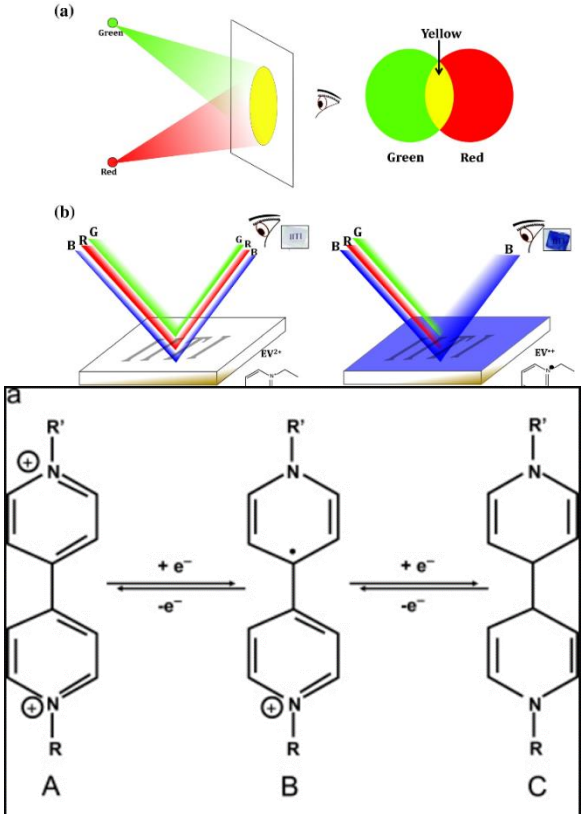

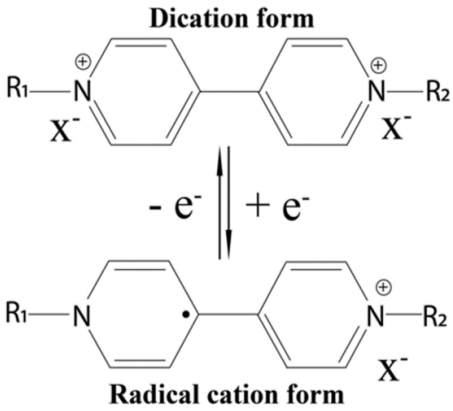

Figure 2.14: Showing various forms of EV which shows color.

2.10 Poly (3-Hexyl thiophene) (P3HT)

Poly(3-hexylthiophene) (P3HT) is a semiconducting polymer widely used in organic electronics. With its conjugated backbone structure, P3HT exhibits excellent electrical conductivity[14] and optical properties[15]. In electrochromic devices, P3HT can reversibly change its color when subjected to an applied voltage or current. This property arises from the polymer's ability to undergo redox reactions, leading to changes in its absorption spectrum. P3HT-based electrochromic materials have been explored for applications in smart windows, displays, and sensors, offering a versatile platform for responsive and energy-efficient optoelectronic devices.

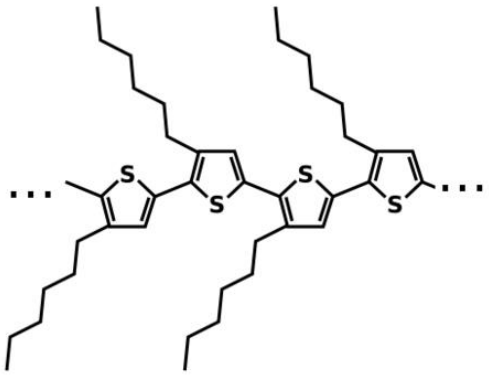

How Poly(3-hexylthiophene) P3HT shows colour:

Poly(3-hexylthiophene), abbreviated as P3HT, is a widely utilized polymer in organic solar cells. Its colouration primarily stems from its electronic structure, particularly the energy levels of its highest occupied molecular orbital (HOMO) [15]and lowest unoccupied molecular orbital (LUMO). The observed colour of P3HT results from the selective absorption and reflection of light at specific wavelengths, dictated by the energy difference between the HOMO and LUMO levels, commonly referred to as the band gap. When light with energy matching this band gap is absorbed, electrons undergo excitation from the HOMO to the LUMO. The remaining wavelengths of light are either transmitted or reflected, contributing to the perceived colour of the material.

2.11 Preparation of thin film for CV

Approximately 1 mg of the metal oxide is dispersed in 2 ml of ethanol and sonicated for 30 minutes to ensure proper mixing. Following this, 5 µl of Nafion is introduced into the solution to serve as a binding agent. Meanwhile, an ITO substrate measuring 2×1 cm^2 is meticulously cleaned using a sonicator to remove any contaminants. Once dried, 100 µl of the prepared solution is drop-cast onto the ITO substrate and allowed to settle undisturbed, facilitating the evaporation of ethanol. Subsequently, the electrode is prepared for various measurements.

Chapter 3

RESULTS AND DISCUSSIONS

Section A

3.1 Basic characterization of the synthesized materials

3.1.1 Zinc Oxide

Zinc oxide (ZnO) is a multifunctional semiconductor material renowned for its diverse applications and unique properties. With a direct wide bandgap of approximately[16] 3.37 eV, ZnO finds utility in optoelectronic devices like LEDs, solar cells, and UV photodetectors. Its exceptional transparency in the visible region makes it suitable for transparent conductive coatings in displays and touchscreens[17]. Moreover, ZnO's piezoelectric properties enable its use in sensors, actuators, and energy harvesting devices. Nanoparticles of ZnO serve in cosmetics, biomedical imaging, and drug delivery systems, thanks to their biocompatibility and photocatalytic activity[18]. ZnO also boasts a significant dielectric constant, enhancing its value in capacitors and other electronic applications[19]. Additionally, its robust antibacterial properties make it ideal for antimicrobial coatings, ensuring its relevance across various industries[20].

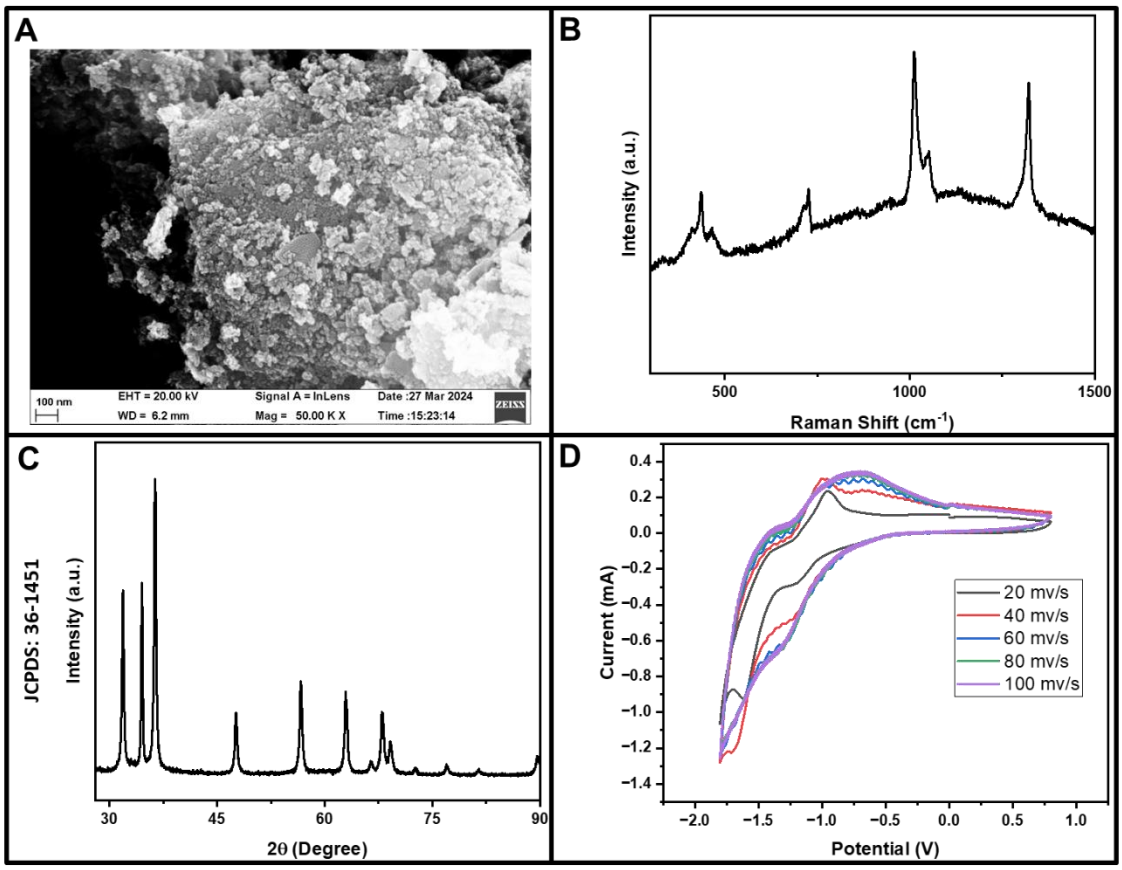

Figure 3.1: (a) SEM image (b) Raman shift (c) XRD (d) Cyclic voltammetry at different scan rates.

SEM images: From the SEM images we can see that very fine particles of less than 100 nm are formed. These fine particles are clustered together to form bigger particles.

Raman spectroscopy: We can see various peaks at 436, 712, 726, 1011, 1051, 1320 cm^{-1}. The peak at 436 cm^{-1} corresponds[21] to E_2^{high} mode. The peaks at 712 and 726 correspond to LA+TO modes i.e Longitudinal Acoustic and Transverse Optical phonon modes. The peak at 1051 corresponds to TO+LO i.e Transverse Optical and Longitudinal Optical phonon modes of vibration. Additionally, Raman scattering from defects, such as oxygen vacancies or zinc interstitials, can result in additional peaks or broadening of existing peaks in the Raman spectrum.

XRD: X-ray diffraction (XRD) analysis of zinc oxide (ZnO) powder shows that it has wurtzite structure, which belongs to the space group P63mc[22], provides valuable insights into its crystalline properties. The wurtzite structure of ZnO is characterized by hexagonal symmetry, with zinc and oxygen atoms arranged in alternating layers along the c-axis. In XRD patterns of ZnO, characteristic diffraction peaks corresponding to the

crystallographic planes (hkl) can be observed, such as[23] (100), (002), and (101). The XRD pattern closely matches with the JCPDS card no 36-1451.

Cyclic voltammetry: The cyclic voltammetry is performed by taking a thin film of ZnO drop casted on ITO in a three electrode setup using[24] 1 M $LiClO_4$ as an electrolyte. The CV curve is recorded in the potential window -1.8 V to 0.8 V. It reveals that there are two oxidation (-0.94 V and -1.4 V) and two reduction (-1.21 V and -1.61 V) peaks. At lower scan rate all the peaks are noticeable. At higher scan rate all the peaks are not distinguishable.

3.1.2 Tungsten trioxide

Tungsten trioxide (WO_3) is a versatile transition metal oxide compound with a wide range of applications owing to its unique properties. It exists in various structural forms, including monoclinic, orthorhombic, and hexagonal phases, each exhibiting distinct physical and chemical characteristics[25]. WO_3 is most commonly found in its monoclinic form, featuring layers of tungsten atoms sandwiched between layers of oxygen atoms. This layered structure contributes to its exceptional electrochromic, photochromic, and catalytic properties.

One of the most notable applications of WO_3 is in electrochromic devices (ECDs), where it serves as an active material capable of reversibly changing its optical properties in response to an applied voltage[26]. This property finds use in smart windows, displays, and electronic devices, enabling dynamic control over light transmission and energy efficiency. Additionally, WO_3 is utilized in gas sensors for detecting harmful gases such as nitrogen dioxide and carbon monoxide due to its high surface area and sensitivity to gas molecules[27].

Furthermore, WO_3 nanoparticles exhibit promising photocatalytic activity, making them suitable for environmental remediation, water purification, and solar energy conversion[28]. WO_3-based materials are also employed in lithium-ion batteries[29], electrochromic mirrors, and electrochromic smart films, showcasing its versatility across various technological domains. Overall, tungsten trioxide's unique properties make it a valuable material for applications ranging from energy storage and conversion to environmental monitoring and optoelectronics.

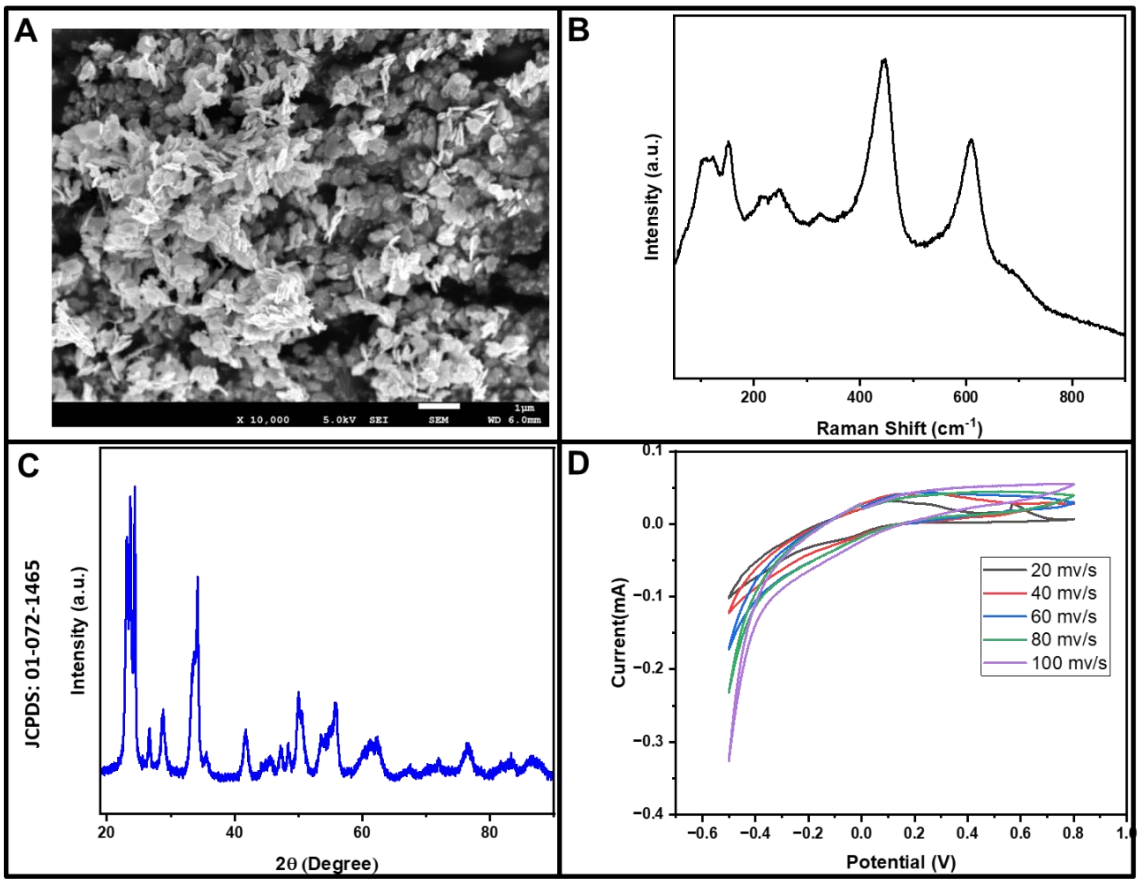

Figure 3.2: (a) SEM image (b) Raman shift (c) XRD (d) Cyclic voltammetry at different scan rates.

SEM images: From the morphology we can say that flakes of 0.5 μm are formed.

Raman spectroscopy: The Raman spectra of tungsten trioxide (WO_3) offer valuable insights into its structural properties and vibrational modes[30]. In the Raman spectrum of WO_3, characteristic peaks arise from the symmetric stretching and bending vibrations of the tungsten-oxygen (W-O) bonds within the crystal lattice. Typically, WO_3 exhibits several prominent Raman peaks in the range of 100 to 1000 cm^{-1}, reflecting its complex crystal structure and symmetry.

XRD: The diffraction peaks observed in the experimental [31]pattern 22◦ (001), 23.4◦ (110), 25◦ (101), 42◦ (220), 55◦ (202) match closely with the positions and intensities of peaks in the reference pattern JCPDS: 01-072-1465. So we can conclude that the synthesized WO_3 is in its monoclinic phase.

Cyclic voltammetry: The cyclic voltammetry is performed by taking a thin film of WO_3 drop casted on ITO in a three electrode setup[32] using 0.5 M H_2SO_4 as an electrolyte. The

CV curve is recorded in the potential window -0.5 V to 0.8 V. It reveals that there is one oxidation (0.13 V) and one reduction (-0.06 V) peak.

3.1.3 Titanium dioxide

Titanium dioxide (TiO_2) is a versatile semiconductor known for its photocatalytic, optical, and electronic properties[33]. It occurs in various crystalline forms, with anatase and rutile being the most common. Anatase TiO_2 exhibits superior photocatalytic activity, finding applications in environmental remediation and self-cleaning surfaces[34]. As a white pigment, TiO_2 is widely used in paints, coatings, plastics, and cosmetics due to its high refractive index and opacity[35]. In sunscreens, TiO_2 nanoparticles provide UV protection by scattering and absorbing ultraviolet radiation. Additionally, TiO_2 plays a vital role in energy storage and conversion technologies, including dye-sensitized solar cells and lithium-ion batteries. Its diverse applications make TiO_2 a key material in industries ranging from environmental engineering and cosmetics to renewable energy and electronics.

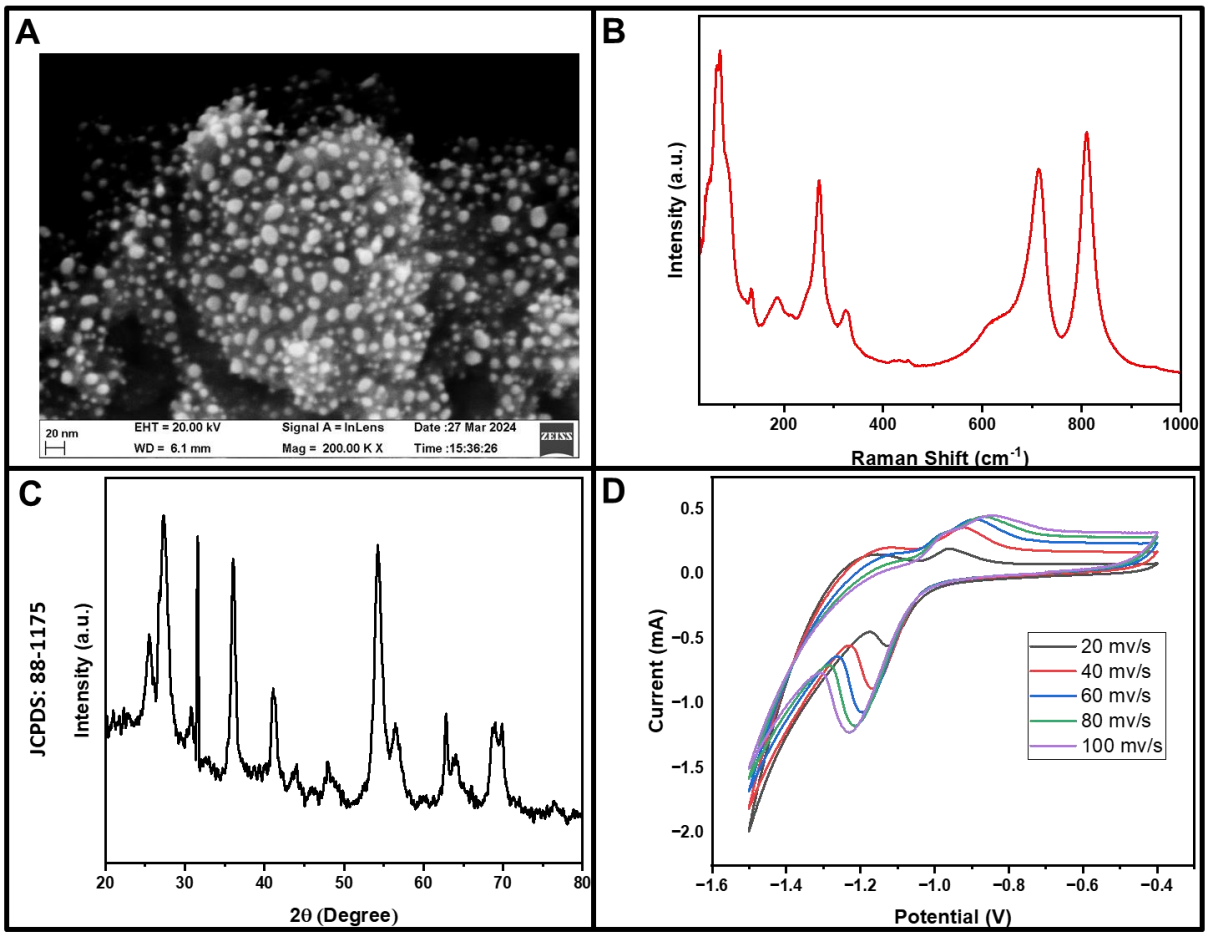

Figure 3.3: (a) SEM image (b) Raman shift (c) XRD (d) Cyclic voltammetry at different scan rates.

SEM images: spherical particles of approx. 20 nm are formed, which are clumped together to form bigger blobs.

Raman spectroscopy: In the Raman spectrum of TiO_2, characteristic peaks[36] correspond to different vibrational modes, offering information about its crystal structure, phase purity, and defects. Typically, TiO2 exhibits prominent Raman bands attributed to its rutile or anatase phases, with peaks corresponding to symmetric stretching modes (E_g), bending modes (E_g, B_{1g}), and oxygen vacancies (Tio-Ti). The raman shift is matched with existing literature. And we can confirm that we have successfully synthesized TiO_2 .

XRD: In the X-ray diffraction (XRD)[37] pattern of TiO_2, characteristic peaks are observed corresponding to its crystalline phases, primarily rutile and anatase. The anatase phase typically exhibits diffraction peaks at 2θ angles of around 25.3°, 37.8°, 48°, and 54.4°, corresponding to the (101), (004), (200), and (105) crystallographic planes, respectively. Similarly, rutile TiO2 displays peaks at approximately 27.4°, 36.1°, and 54.3°, corresponding to the (110), (101), and (211) planes. The relative intensities and positions of these peaks can vary depending on factors such as sample preparation methods and annealing conditions. Additionally, the presence of other phases or impurities may result in additional peaks in the XRD pattern. The XRD pattern matches closely with the JCPDS card no 88-1175 confirming the successful synthesis of TiO_2 particles.

Cyclic voltammetry: The cyclic voltammetry is performed by taking[38] a thin film of TiO_2 drop casted on ITO in a three electrode setup using 0.1 M KCl as an electrolyte. The CV curve is recorded in the potential window -1.5 V to -0.4 V. It reveals that there is one oxidation (-0.92 V) and one reduction (-1.17 V) peak. Slowing drifting peaks show pseudo reversibility.

3.1.4 Molybdenum trioxide

Molybdenum trioxide (MoO3) is a transition metal oxide with various applications owing to its unique properties. It exists in several crystalline forms, including α-MoO3 and β-MoO3, each exhibiting different physical and chemical characteristics[39]. MoO3 is commonly used as a catalyst in chemical reactions, particularly in the petroleum industry for sulfur removal and in the production of polymers and fine chemicals. It also finds application as an electrochromic material in smart windows, displays, and electronic devices, where it can reversibly change its optical properties in response to an applied voltage. Additionally, MoO3 is utilized in lithium-ion batteries as an electrode material due to its high capacity and stability. Furthermore, MoO3 nanoparticles show promising potential in gas sensing, photovoltaics, and photoelectrochemical water splitting for renewable energy applications. Overall, molybdenum trioxide's diverse properties make it a valuable material for a wide range of industrial and technological applications.

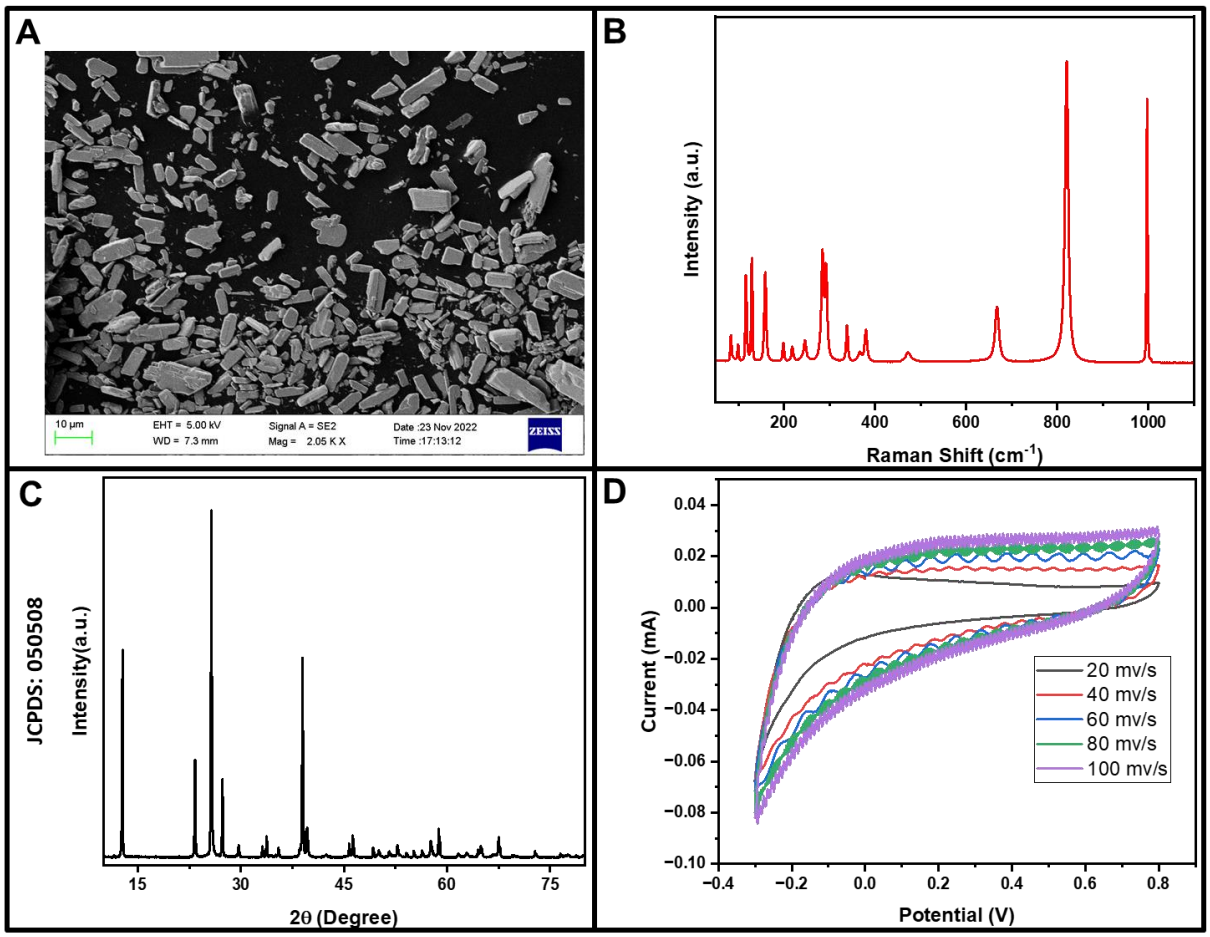

Figure 3.4: (a) SEM image (b) Raman shift (c) XRD (d) Cyclic voltammetry at different scan rates.

SEM images: MoO_3 particles of approximate 10µm are formed.

Raman spectroscopy: In molybdenum trioxide (MoO3), Raman modes indicate how its atoms vibrate. These modes are like fingerprints, showing unique vibrations. The spectra reveal different peaks at specific frequencies[40]. For example, peaks at 996 cm−1 and 817 cm−1 show certain stretching motions, while others at 667 cm−1 and 471 cm−1 indicate bending. These peaks help identify the structure and properties of MoO3. The observed spectrum is matched with the existing literature on MoO_3.

XRD: Matched [9]with the JCPDS card no 050508.

Cyclic voltammetry: The cyclic voltammetry is performed by [41]taking a thin film of MoO_3 drop casted on ITO in a three electrode setup using 1 M $LiClO_4$ as an electrolyte. The CV curve is recorded in the potential window -0.3 V to 0.8 V.

3.2 EIS of single electrode

EIS is performed using a three electrode setup as shown in the picture below. The measurement is performed at different voltages as indicated in the respective diagrams. The setup and the electrolyte for performing the EIS experiment is same as the set up for recording CV.

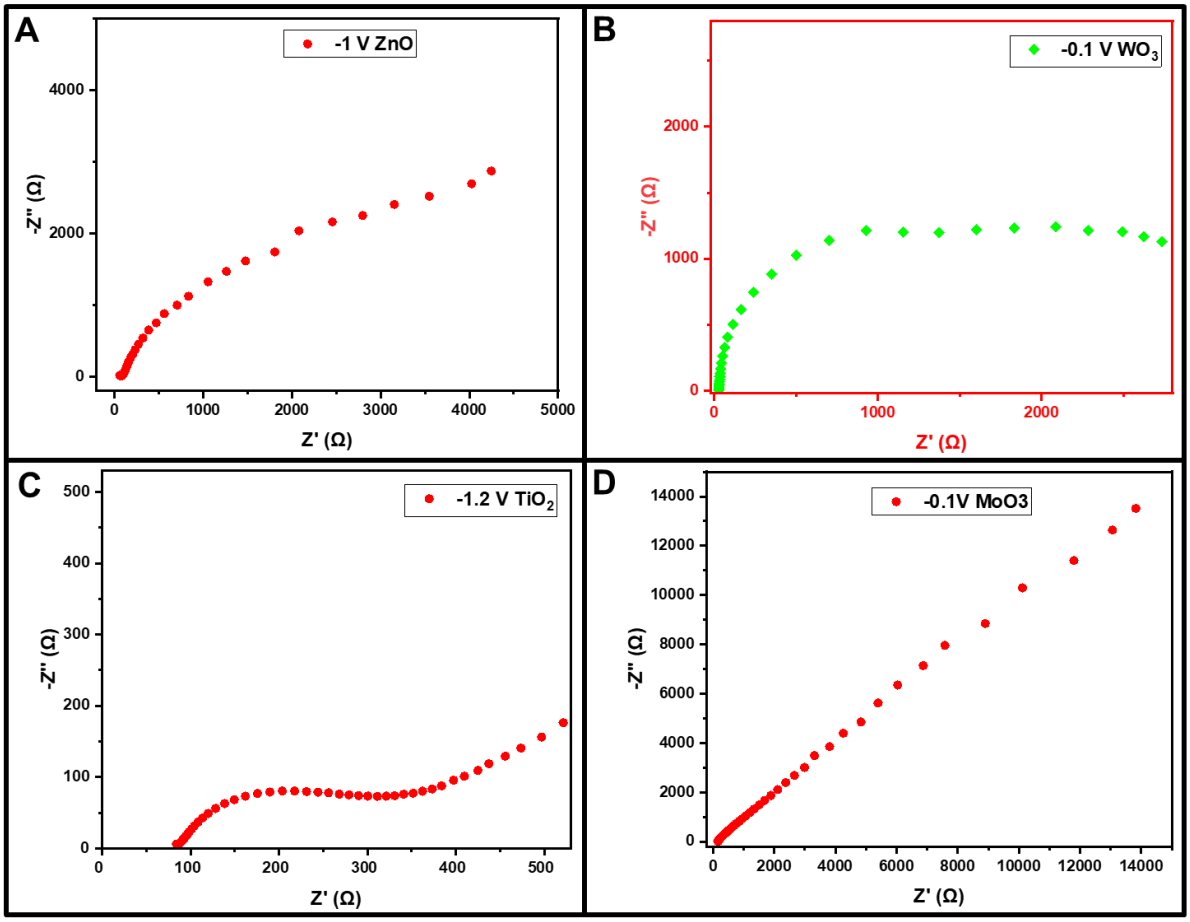

Figure 3.5: (a) ZnO at -1 V (b) WO_3 at -0.1 V (c) TiO_2 at -1.2 V (d) MoO_3 at -0.1 V

Electrochemical impedance spectroscopy (EIS) provides insights into various electrochemical processes, including the resistive and diffusive nature of the system. In an EIS spectrum, the resistive behavior is reflected in the real part of the impedance (Z'), while the diffusive behavior is evident in the imaginary part (Z''). A high frequency semicircle in the Nyquist plot indicates the charge transfer resistance (R_{ct}), [42]which reflects the resistive nature of the interface. The Warburg element or inclined line at lower frequencies suggests the diffusive nature, representing the transport of ions within the electrolyte or electrode material. Additionally, changes in the shape and position of impedance plots can indicate alterations in the electrochemical processes, such as changes in reaction kinetics, interface properties, or ion diffusion coefficients.

Section B

3.3 CV and EIS of combined systems

The samples mentioned above were drop-cast onto ITO substrates, after which measurements were conducted using a three-electrode setup. Subsequently, the drop-cast films were immersed in EV solution, and all measurements were carried out accordingly. All the EIS measurements are carried out at 0 V.

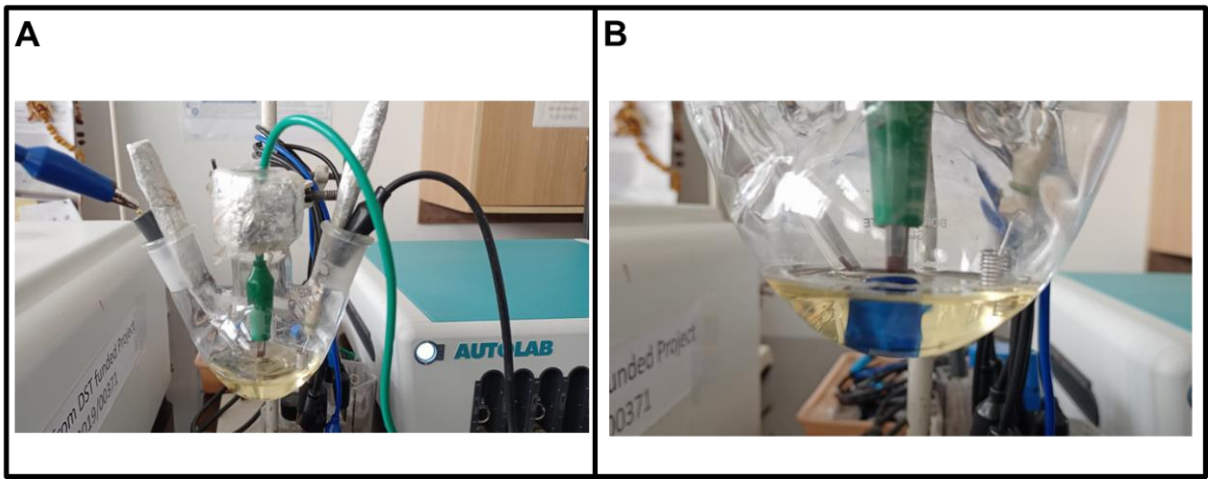

Figure 3.6: Three electrode setup. And how we performed the CV and EIS of combined system.

3.3.1 EV+ITO

This serves as the control setup, where we conducted CV and EIS on a bare ITO electrode immersed in the EV solution.

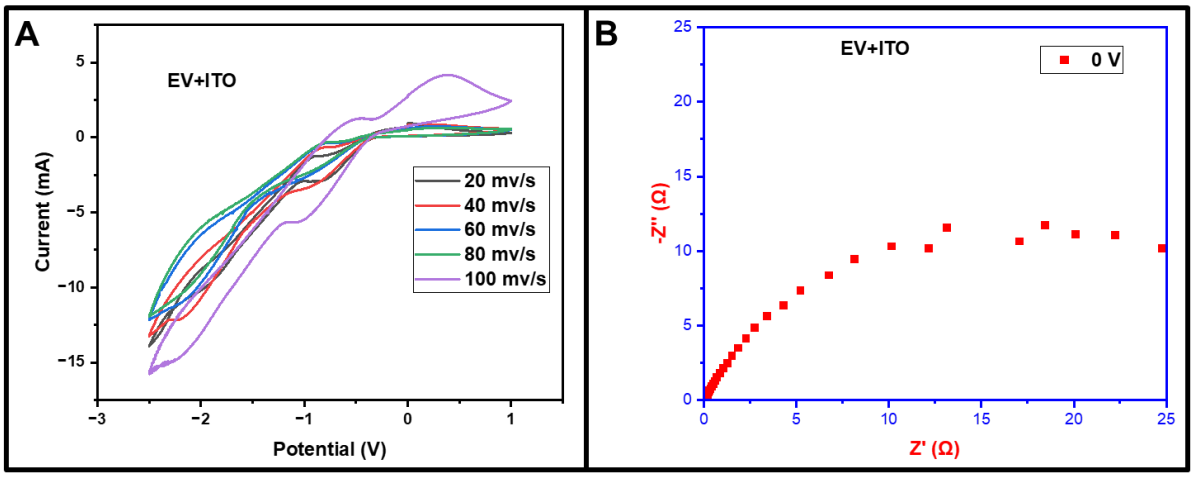

Figure 3.7: (a) CV of EV at different scan rates (b) EIS measurement at 0 V

3.3.2 ZnO+ITO+EV

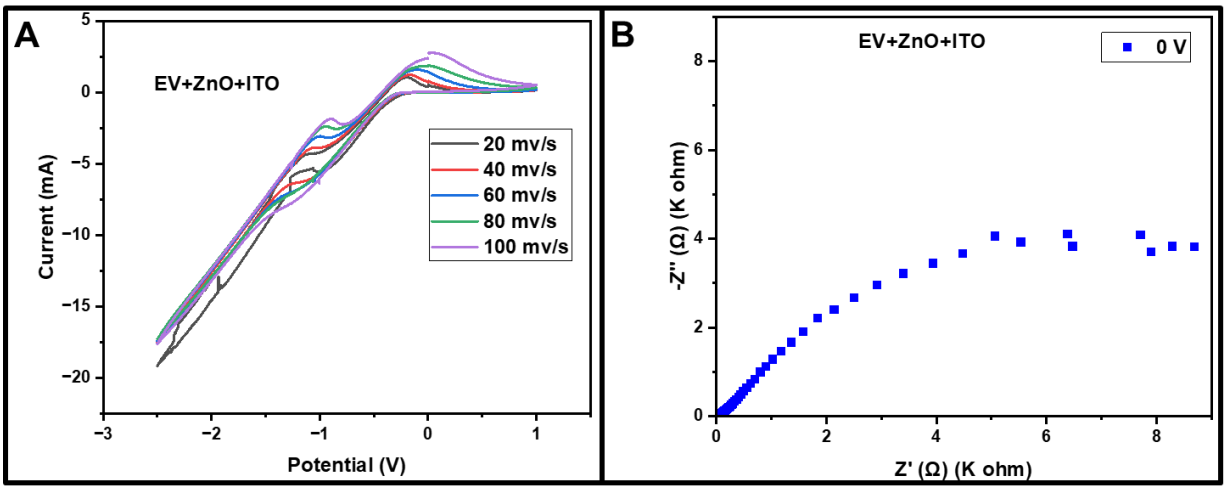

Figure 3.8: (a) CV of ZnO film dipped in EV at different scan rates (b) EIS measurement of the system at 0 V

3.3.3 WO_3+ITO+EV

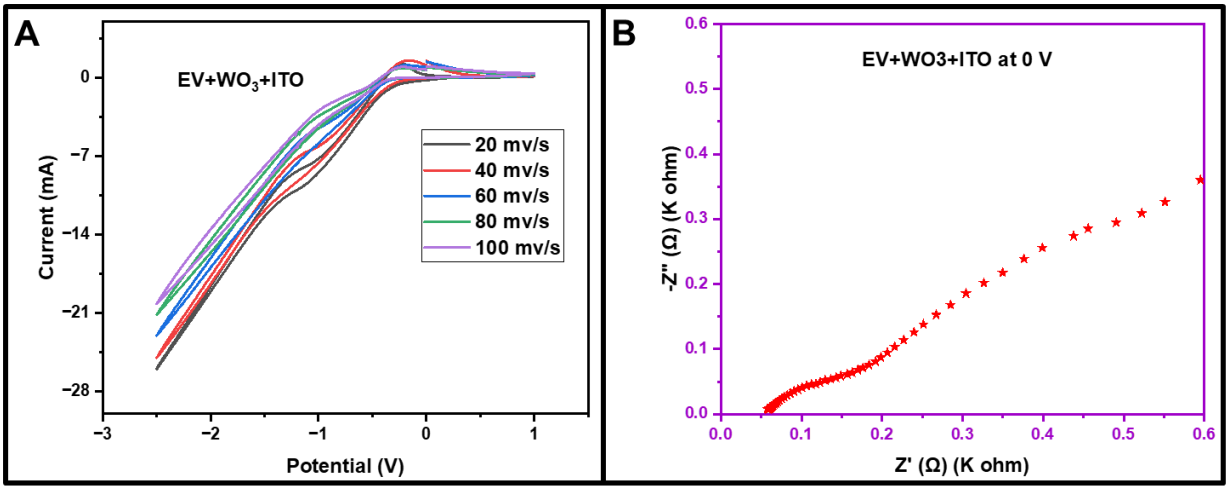

Figure 3.9: (a) CV of WO_3 film dipped in EV at different scan rates (b) EIS measurement of the system at 0 V

3.3.4 TiO_2+ITO+EV

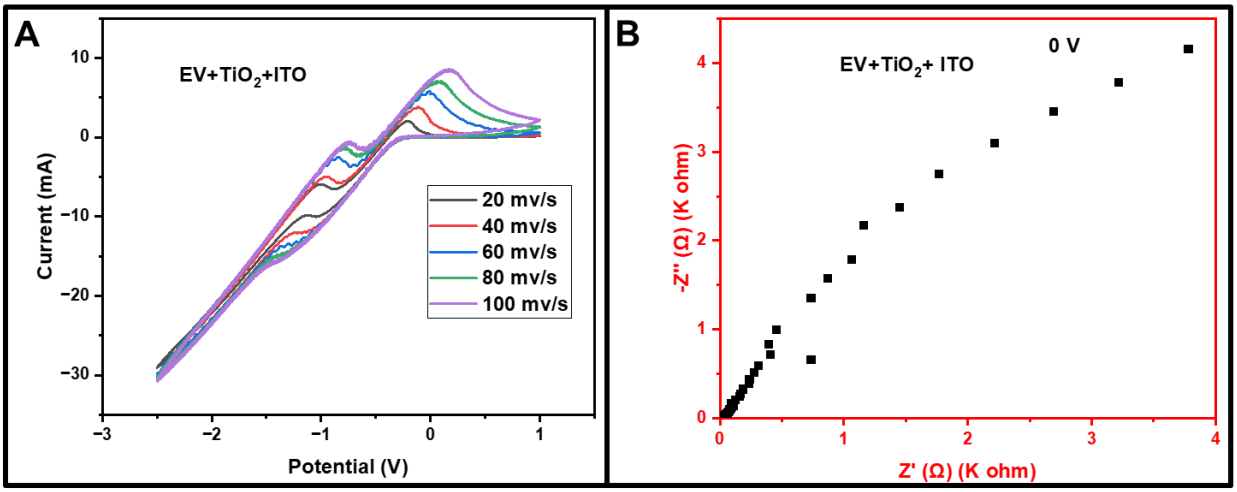

Figure 3.10: ((a) CV of TiO_2 film dipped in EV at different scan rates (b) EIS measurement of the system at 0 V

3.3.5 MoO_3+ITO+EV

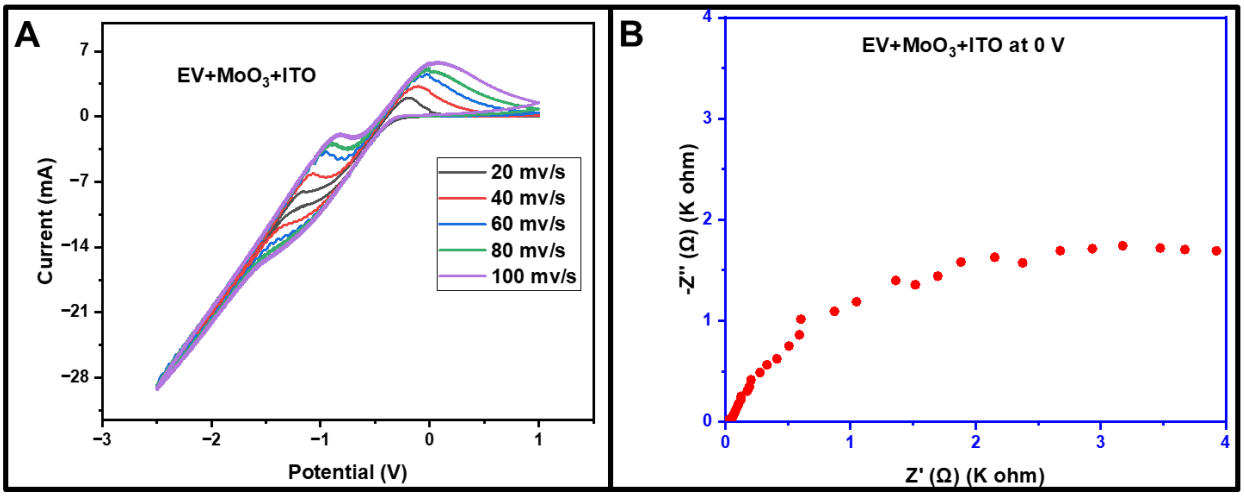

Figure 3.11: (a) CV of MoO_3 film dipped in EV at different scan rates (b) EIS measurement of the system at 0 V

Section C

3.4 Device performance

Following the fabrication method outlined in Chapter 2, we proceeded to assess the device across several parameters including coloration time (T_c), bleaching time (T_b), stability, and coloration efficiency at two wavelengths, namely 515nm and 750nm.

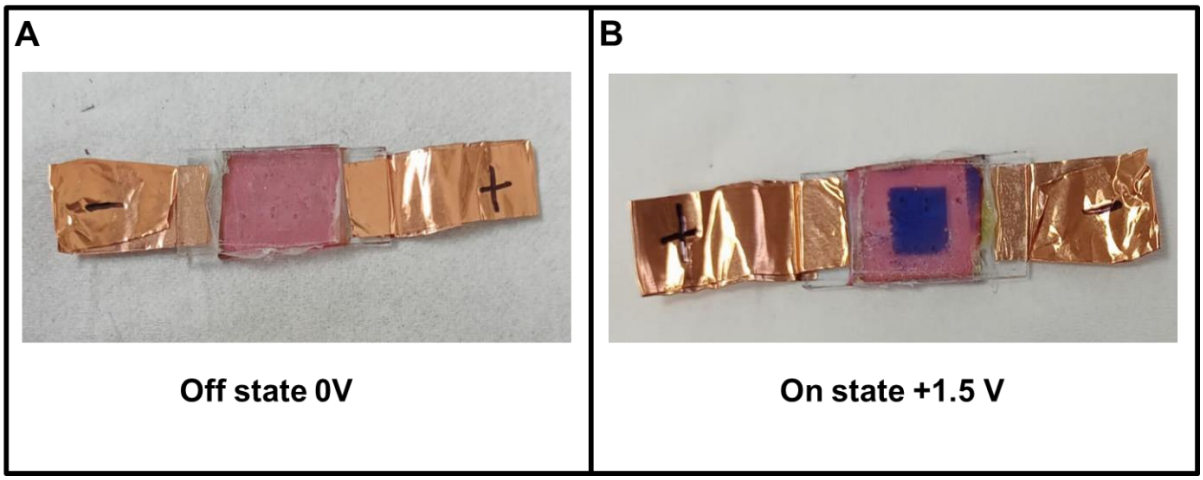

Figure 3.12: Electrochromic device

3.4.1 EV+P3HT

From the % transmittance data, it is evident that significant changes in % transmittance occur at wavelengths of 515 nm and 750 nm. Hence, all measurements were conducted at these wavelengths. Graph A illustrates that the lines corresponding to 0 V and -1.5 V almost overlap, indicating good reversibility of the device. To determine the switching time at 515 nm, absorbance values were recorded at intervals of 0.2 s using square pulses of +1.5 V and -1.5 V,

and the time taken to achieve 90% of the maximum transmittance values was noted. Stability was assessed by applying square pulses of +1.5 V (5 seconds) and -1.5 V (5 seconds) over 100 cycles (1000 seconds total). Coloration efficiency was calculated using the formula outlined in Chapter 1. Charge density was determined by dividing the total charge intercalated/deintercalated by the area of the window (1 cm^2). Additionally, color contrast at these wavelengths was computed using the formula provided in Chapter 1.

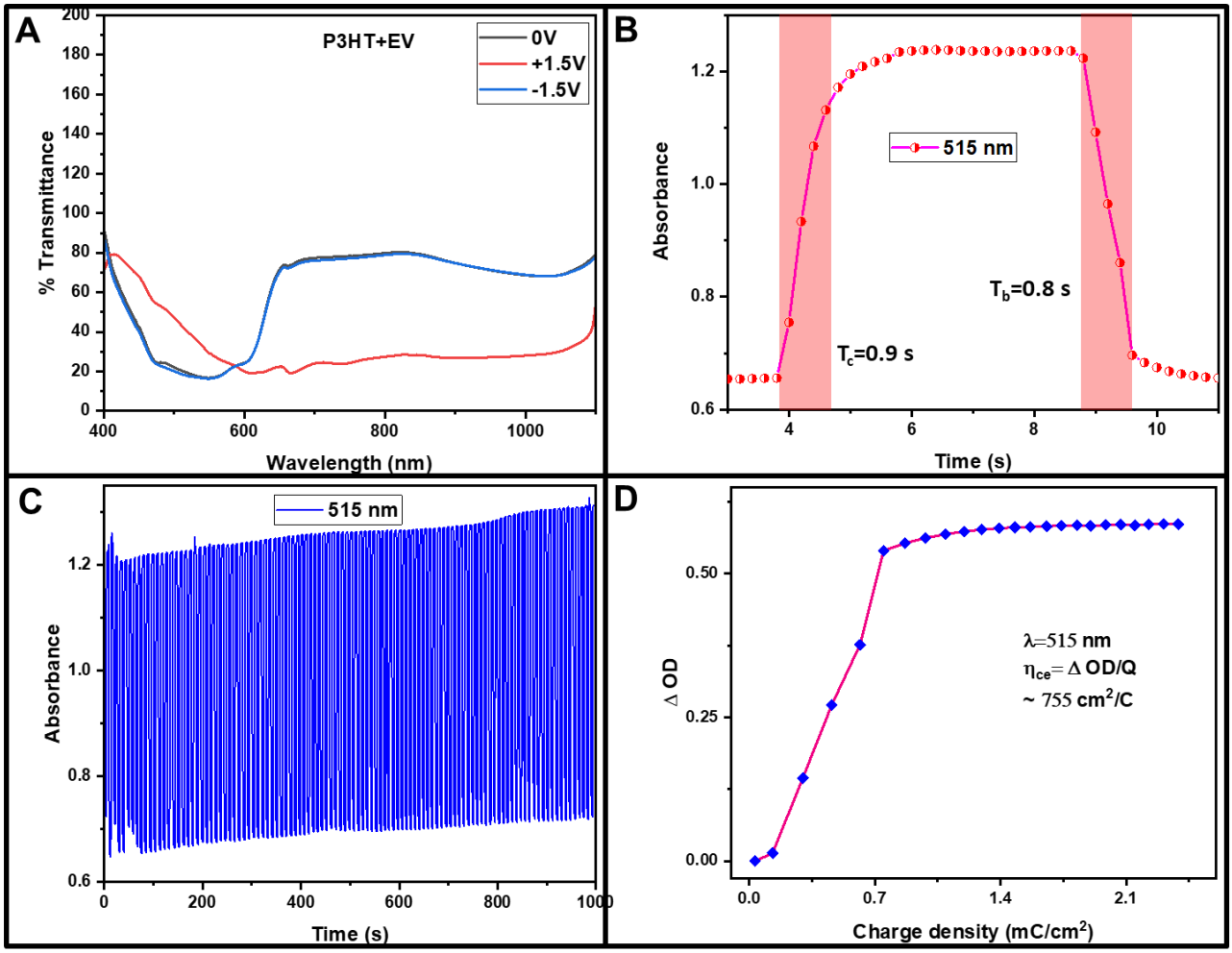

Figure 3.13: (a) Transmittance of the device wrt wavelength at three different voltages 0, +1.5 and -1.5 volts (b) switching at 515 nm (c) Stability at 515 nm (d) Coloration efficiency at 515 nm

For all the other device the data acquisition process is identical. So, I have merely pasted the data. And at the end I have provided a comparison table between various devices and various parameters.

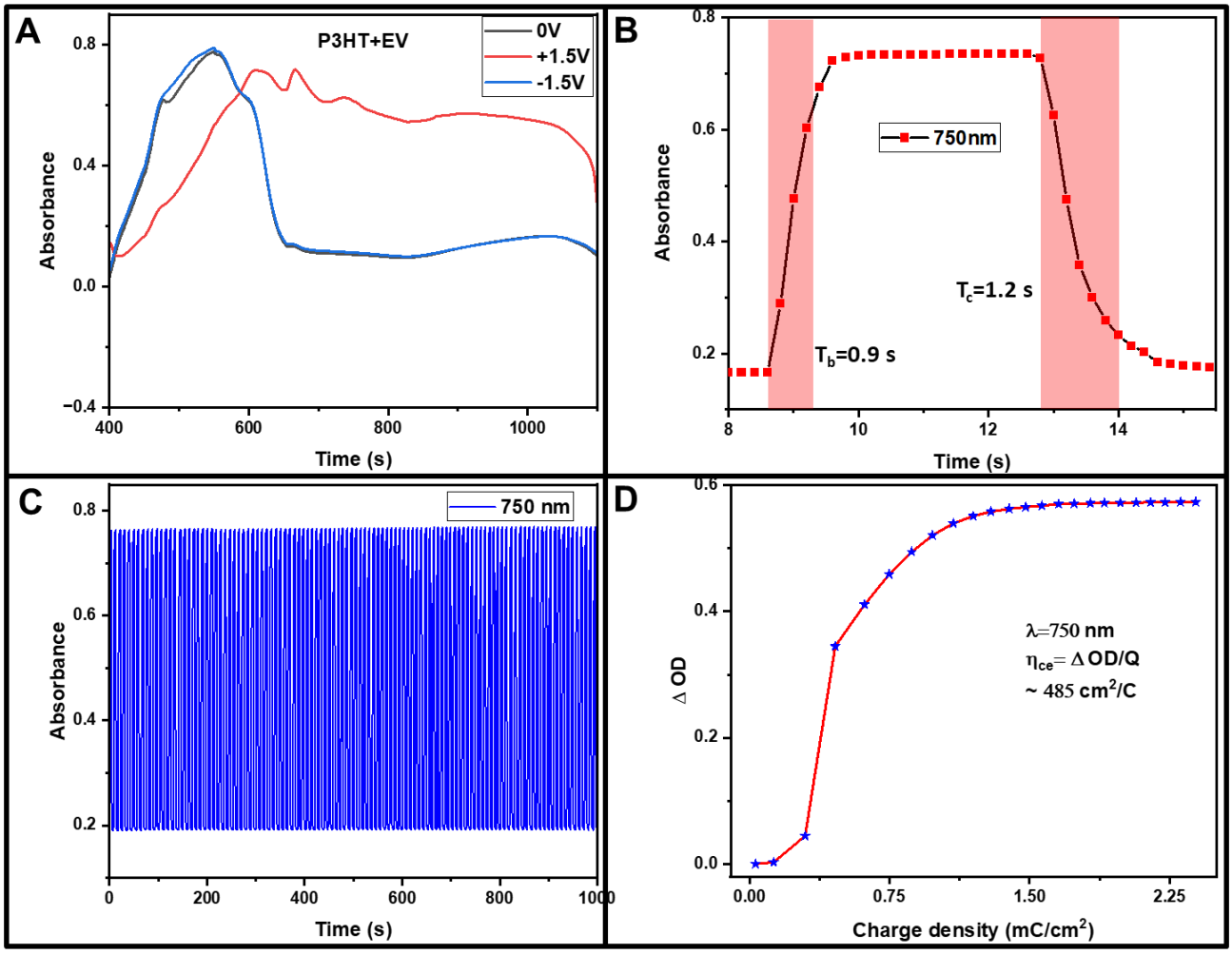

Figure 3.14: (a) Absorbance of the device wrt wavelength at three different voltages 0, +1.5 and -1.5 volts (b) switching at 750 nm (c) Stability at 750 nm (d) Coloration efficiency at 750 nm

Color Contrast at 515 nm= 56 % . Change in transmittance at 750 nm= 52.8 %.

Switching at 515 nm T_c=0.9 s T_b=0.8 s

Switching at 750 nm T_c=1.2 s T_b=0.9 s

Coloration efficiency at 515 nm=755 cm^2/C

Coloration efficiency at 750 nm=755 cm^2/C

Reversibility: Second best

Stability: Best

3.4.2 ZnO+EV+P3HT

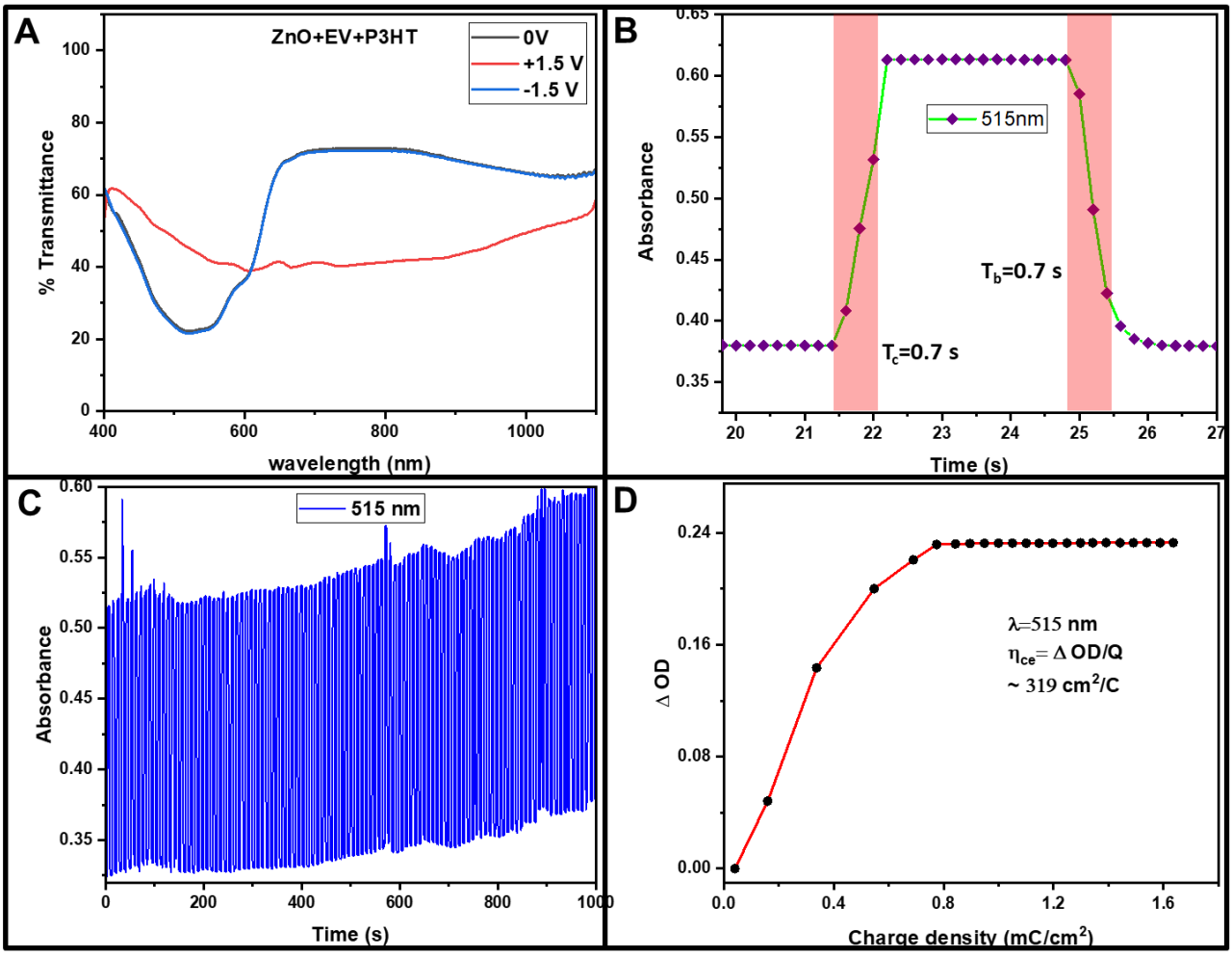

Figure 3.15: (a) Transmittance of the device wrt wavelength at three different voltages 0, +1.5 and -1.5 volts (b) switching at 515 nm (c) Stability at 515 nm (d) Coloration efficiency at 515 nm

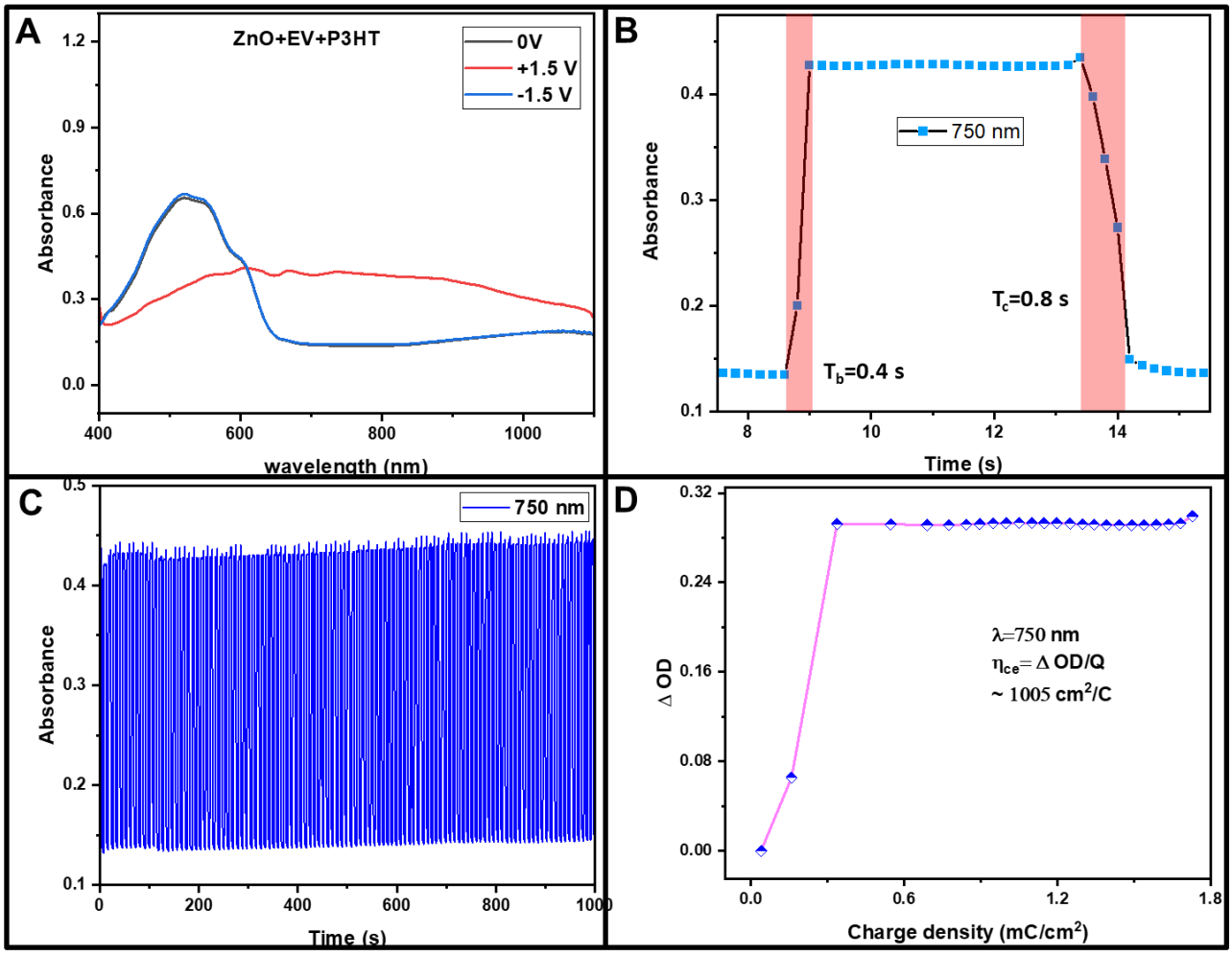

Figure 3.16: (a) Absorbance of the device wrt wavelength at three different voltages 0, +1.5 and -1.5 volts (b) switching at 750 nm (c) Stability at 750 nm (d) Coloration efficiency at 750 nm

Color Contrast at 515 nm= 57.2 % . Change in transmittance at 750 nm= 37.5 %.

Switching at 515 nm T_c=0.7 s T_b=0.7 s

Switching at 750 nm T_c=0.8 s T_b=0.4 s

Coloration efficiency at 515 nm=319 cm^2/C

Coloration efficiency at 750 nm=1005 cm^2/C

Reversibility: Best

Stability: Not so good

3.4.3 WO_3+EV+P3HT

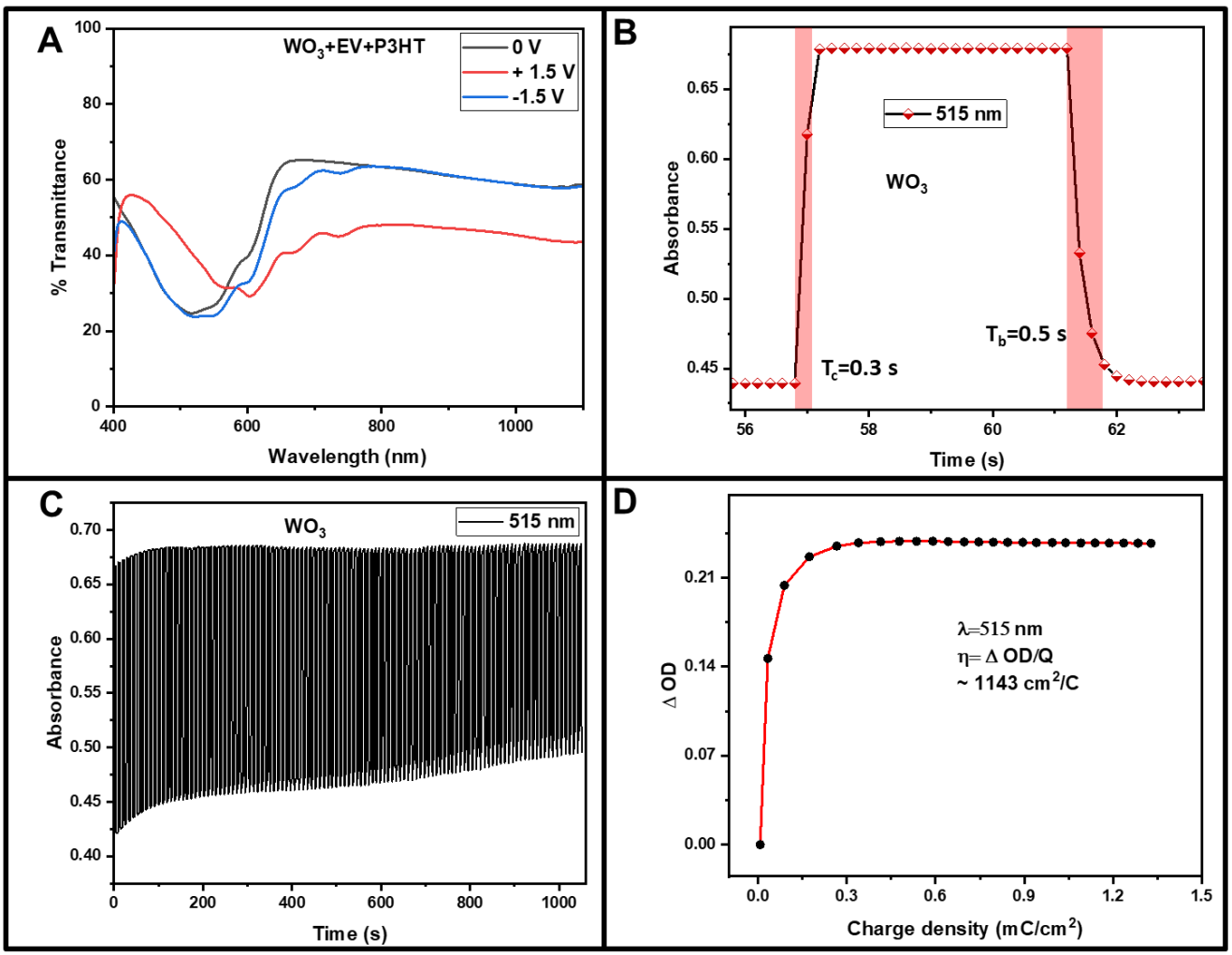

Figure 3.17: (a) Transmittance of the device wrt wavelength at three different voltages 0, +1.5 and -1.5 volts (b) switching at 515 nm (c) Stability at 515 nm (d) Coloration efficiency at 515 nm

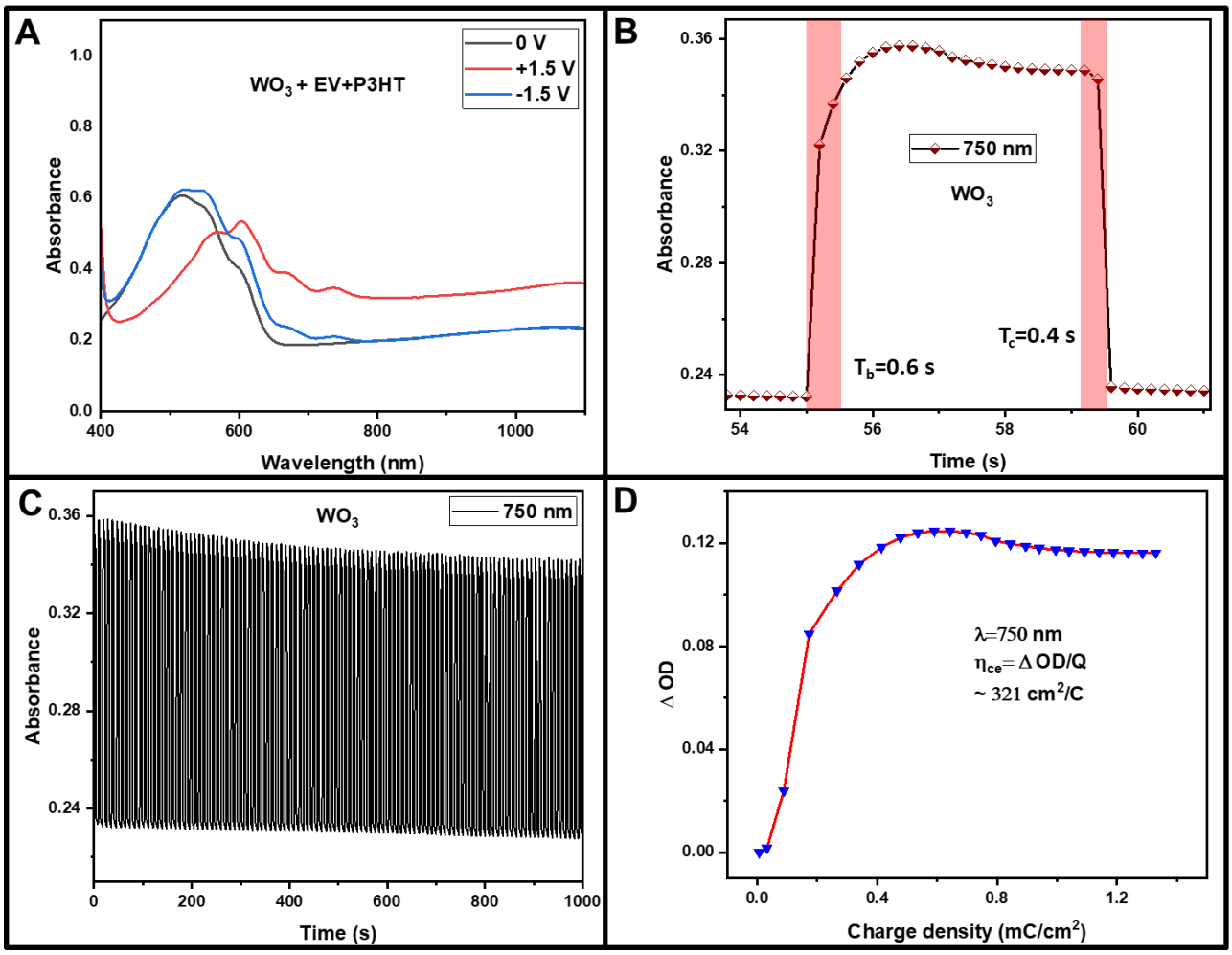

Figure 3.18: (a) Absorbance of the device wrt wavelength at three different voltages 0, +1.5 and -1.5 volts (b) switching at 750 nm (c) Stability at 750 nm (d) Coloration efficiency at 750 nm

Color Contrast at 515 nm= 41.5 % . Change in transmittance at 750 nm= 16.4 %.

Switching at 515 nm T_c=0.3 s T_b=0.5 s

Switching at 750 nm T_c=0.4 s T_b=0.6 s

Coloration efficiency at 515 nm=1143 cm^2/C

Coloration efficiency at 750 nm=321 cm^2/C

Reversibility: poor

Stability: poor

3.4.4 TiO_2+EV+P3HT

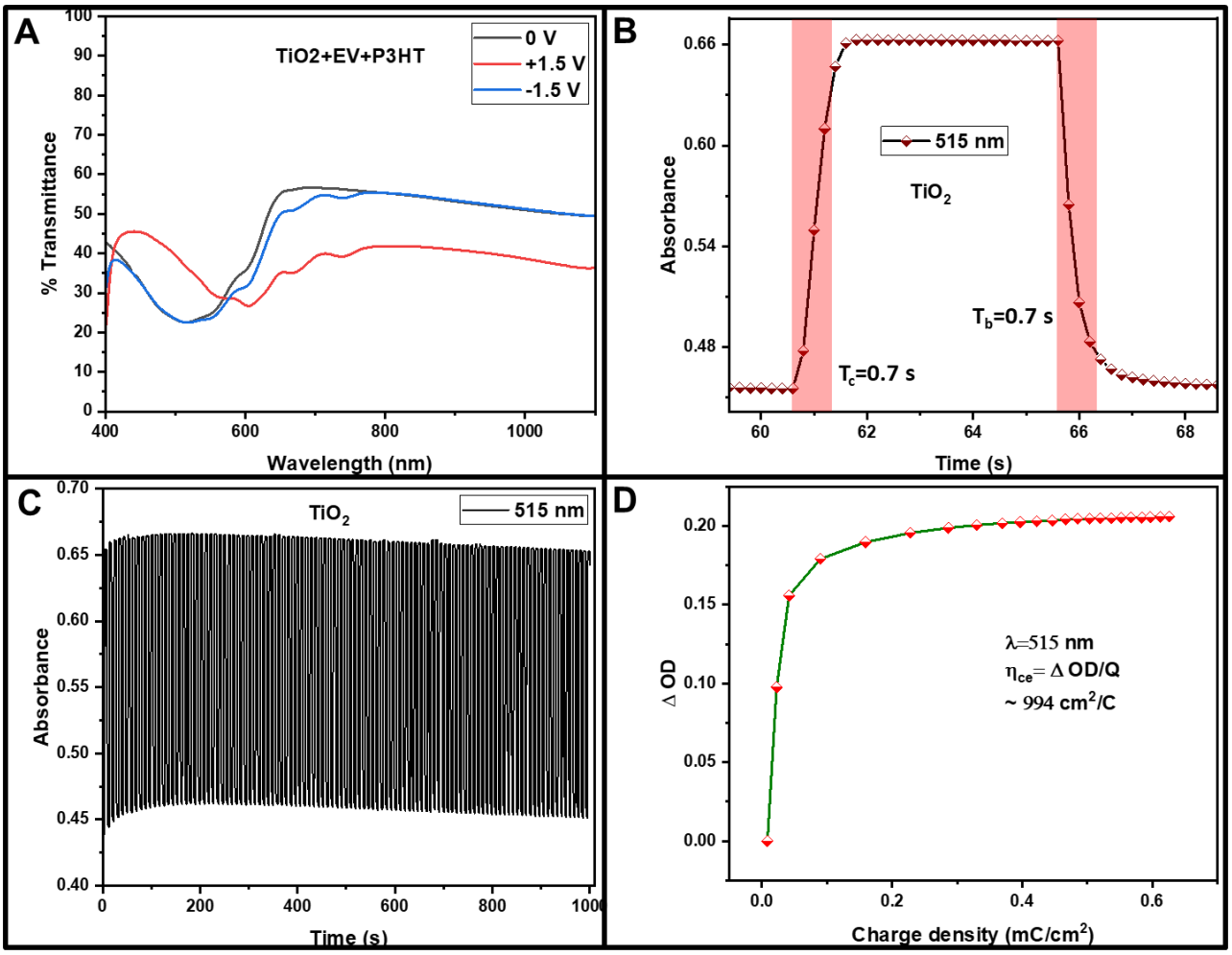

Figure 3.19: (a) Transmittance of the device wrt wavelength at three different voltages 0, +1.5 and -1.5 volts (b) switching at 515 nm (c) Stability at 515 nm (d) Coloration efficiency at 515 nm

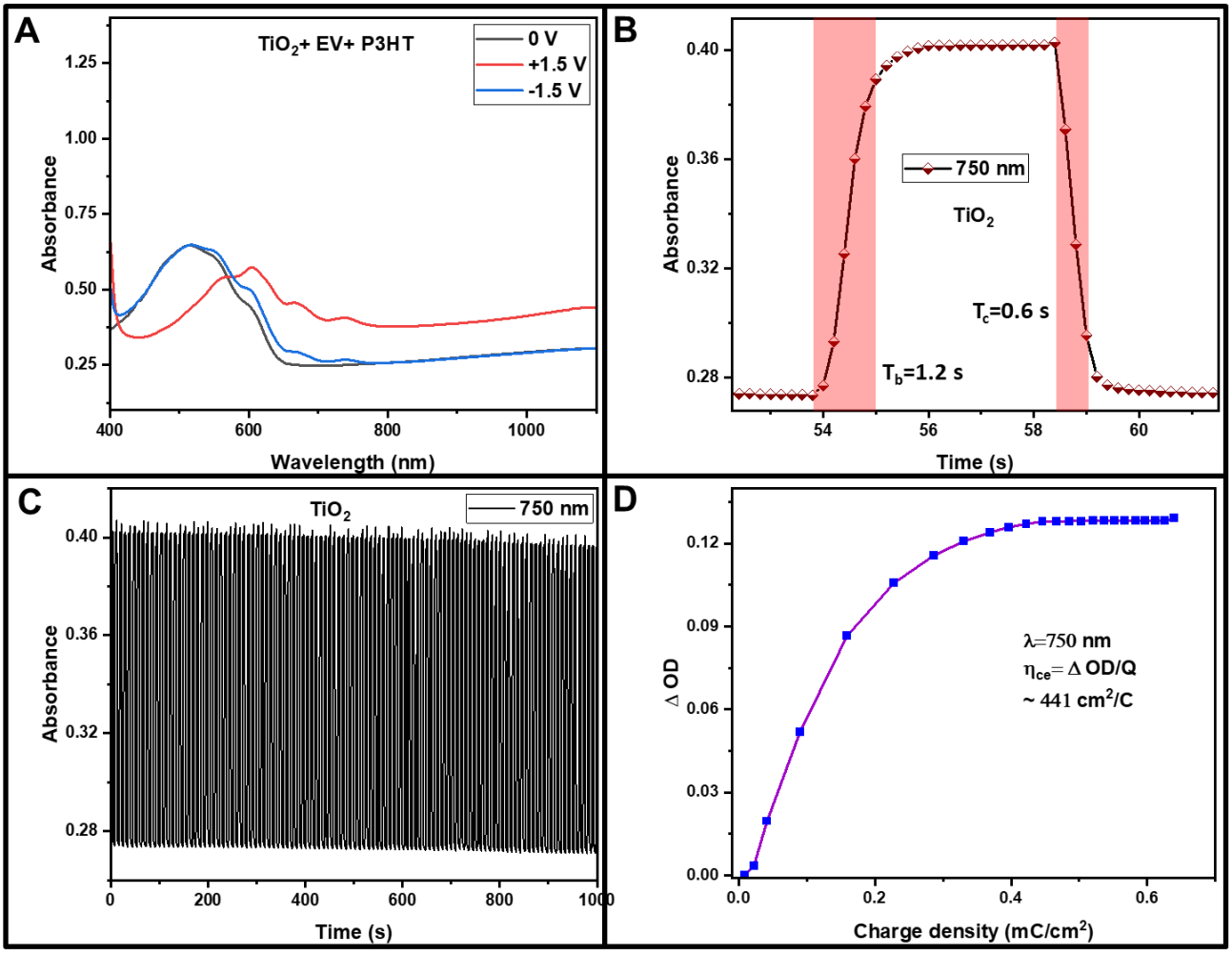

Figure 3.20: (a) Absorbance of the device wrt wavelength at three different voltages 0, +1.5 and -1.5 volts (b) switching at 750 nm (c) Stability at 750 nm (d) Coloration efficiency at 750 nm

Color Contrast at 515 nm= 39 % . Change in transmittance at 750 nm= 14.5 %.

Switching at 515 nm T_c=0.7 s T_b=0.7 s

Switching at 750 nm T_c=0.6 s T_b=1.2 s

Coloration efficiency at 515 nm=994 cm^2/C

Coloration efficiency at 750 nm=441 cm^2/C

Reversibility: Moderate

Stability: Decent

3.4.5 MoO_3+EV+P3HT

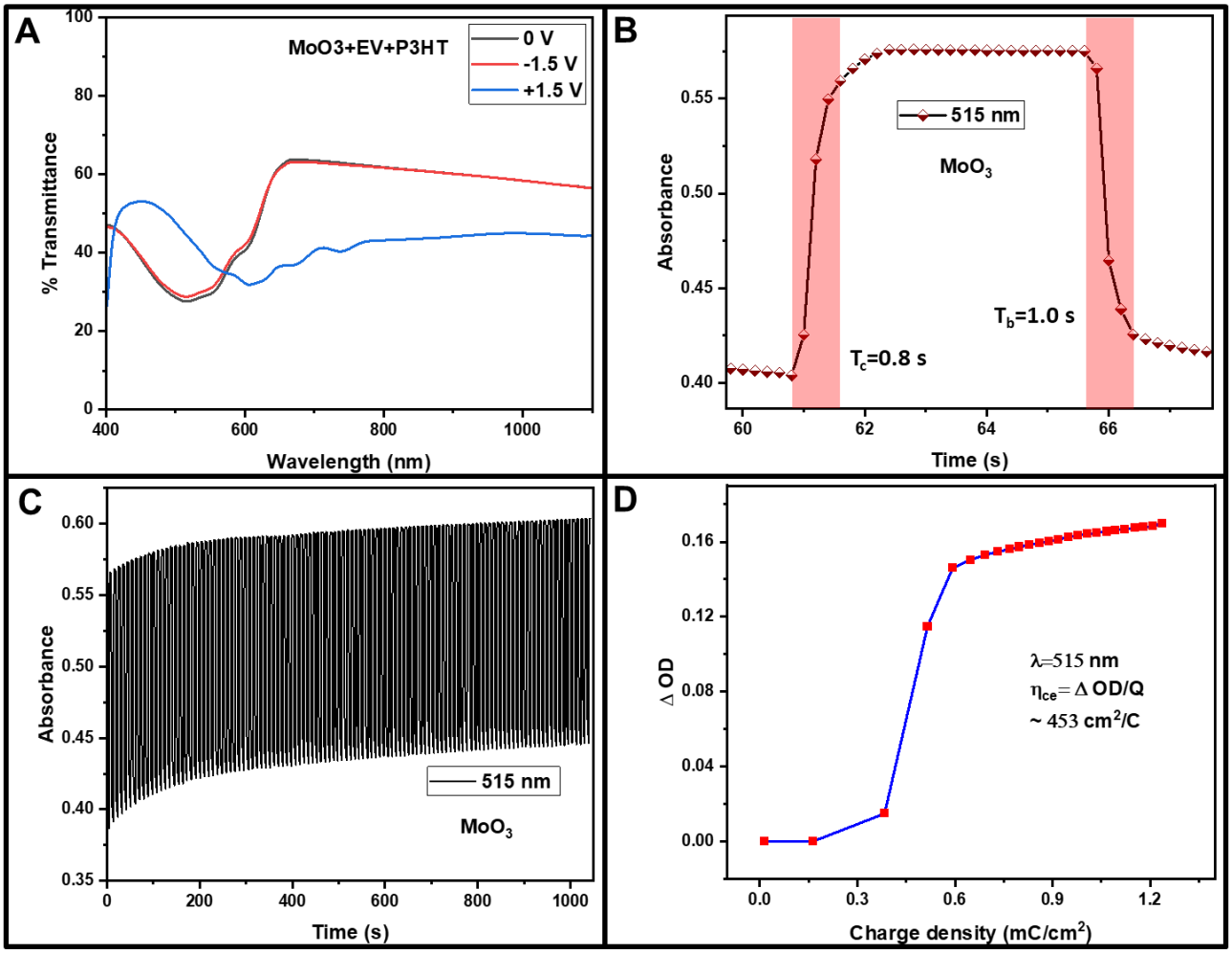

Figure 3.21: (a) Transmittance of the device wrt wavelength at three different voltages 0, +1.5 and -1.5 volts (b) switching at 515 nm (c) Stability at 515 nm (d) Coloration efficiency at 515 nm

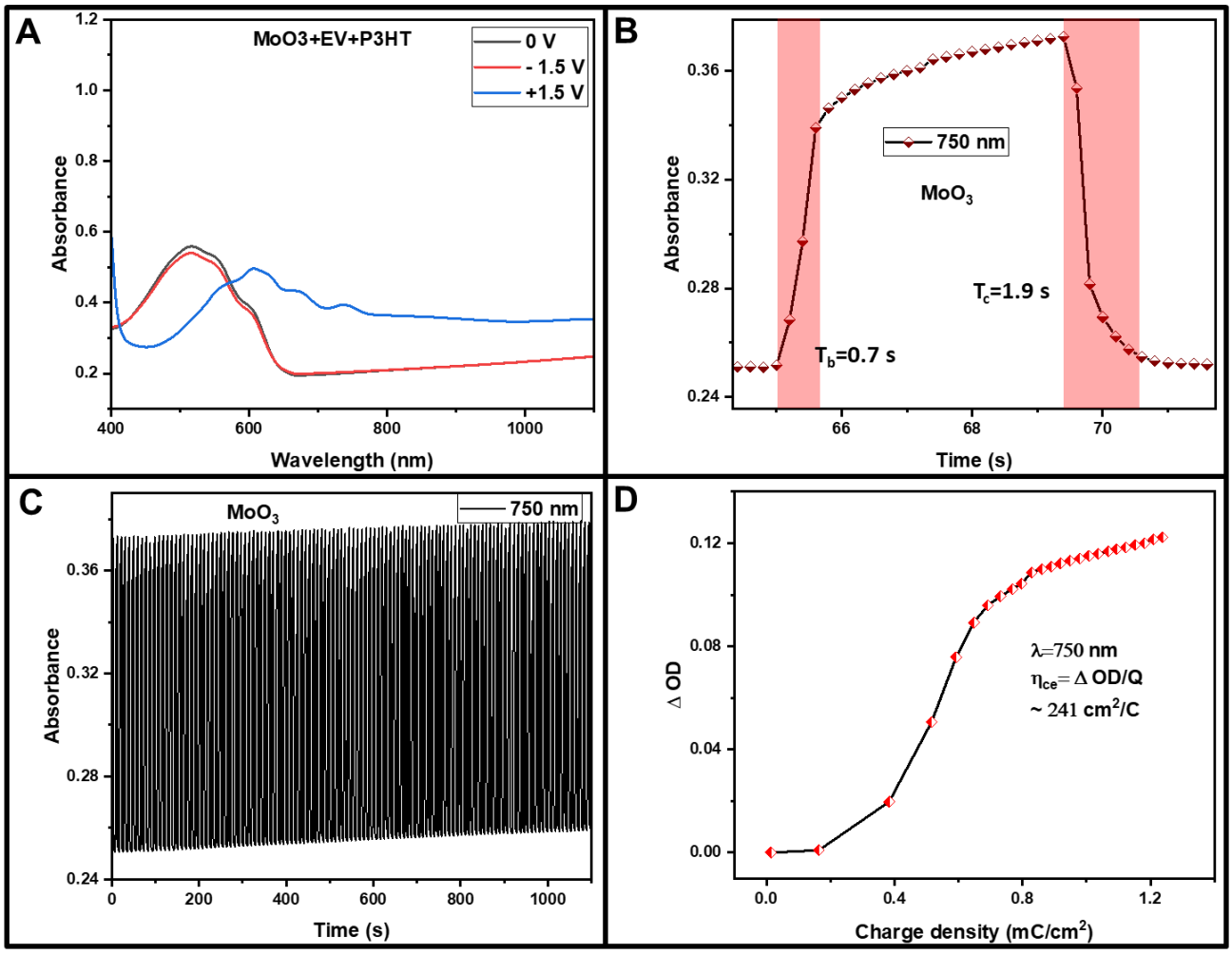

Figure 3.22: (a) Absorbance of the device wrt wavelength at three different voltages 0, +1.5 and -1.5 volts (b) switching at 750 nm (c) Stability at 750 nm (d) Coloration efficiency at 750 nm

Color Contrast at 515 nm= 35.5 % . Change in transmittance at 750 nm= 21.3 %.

Switching at 515 nm T_c=0.8 s T_b=1.0 s

Switching at 750 nm T_c=1.9 s T_b=0.7 s

Coloration efficiency at 515 nm=453 cm^2/C

Coloration efficiency at 750 nm=241 cm^2/C

Reversibility: Good

Stability: Good

Chapter 4

CONCLUSIONS AND FUTURE SCOPE

	P3HT+EV	ZnO+P3HT+EV	WO3+P3HT+EV	TiO2+P3HT+EV	MoO3+P3HT+EV
Switching at 515 nm	Tc= 0.9 s Tb= 0.8 s	Tc= 0.7 s Tb= 0.7 s	Tc= 0.3 s Tb= 0.5 s	Tc= 0.7 s Tb= 0.7 s	Tc= 0.8 s Tb= 1.0 s
Switching at 750 nm	Tc= 1.2 s Tb= 0.9 s	Tc= 0.8 s Tb= 0.4 s	Tc= 0.4 s Tb= 0.6 s	Tc= 0.6 s Tb= 1.2 s	Tc= 1.9 s Tb= 0.7 s
CC at 515 nm (Colour Contrast)	56 %	57.2 %	41.5 %	39 %	35.5 %
ΔT at 750 nm	52.8 %	37.5%	16.4 %	14.5 %	21.3 %
Colouration efficiency (515 nm)	755 cm^2/C	319 cm^2/C	1143 cm^2/C	994 cm^2/C	453 cm^2/C
Colouration efficiency (750 nm)	485 cm^2/C	1005 cm^2/C	321 cm^2/C	441 cm^2/C	241 cm^2/C
Reversibility	Second best	Best			
Stability	Best			Second best	

Table 4.1: Performance table of all the fabricated devices

The data presented in the table provides valuable insights into the performance of various devices fabricated using different doping materials. Upon analysis, it becomes evident that the WO_3-doped device exhibits superior performance in terms of switching and coloration efficiency specifically at a wavelength of 515 nm. Conversely, the ZnO-doped device demonstrates exceptional color contrast at 515 nm. Interestingly, the bare P3HT+EV device emerges as the top performer in terms of stability and percentage modulation at 750 nm. Remarkably, the ZnO-doped device stands out once again, showcasing remarkable coloration efficiency at 750 nm and reversibility, the latter indicating its ability to revert to its original state without any residual color once the voltage is removed. Overall, the ZnO-doped device emerges as the frontrunner across multiple parameters, suggesting its versatility and efficacy.

Moreover, this research offers valuable insights into potential strategies for enhancing specific parameters by doping the P3HT+EV device with appropriate materials, thereby providing a roadmap for further optimization and improvement in device performance.

Future scope

Given the promising results observed with ZnO doping, it is prudent to explore whether the synthesis of ZnO using various methods influences its performance. Methods such as electrodepositing ZnO film, depositing the electroactive form of ZnO, or utilizing the hydrothermal method can yield different morphologies, potentially impacting electron transfer kinetics and consequently altering device performance significantly. Therefore, investigating these different synthesis methods holds immense potential for enhancing our understanding of ZnO-based devices and optimizing their performance characteristics.

- Electrodepositing ZnO on ITO and conducting a thorough characterization of the resulting material.
- Deposition of ZnO on ITO through a hydrothermal process and conducting a thorough characterization of the resulting material.
- Constructing a device wherein ZnO is electrodeposited or hydrothermally grown on ITO, followed by a performance analysis in comparison with a device incorporating powdered ZnO.

References

(1) Kumar, R.; Pathak, D. K.; Chaudhary, A. Current Status of Some Electrochromic Materials and Devices: A Brief Review. *J. Phys. Appl. Phys.* **2021**, *54* (50), 503002. https://doi.org/10.1088/1361-6463/ac10d6.

(2) Chaudhary, A.; Pathak, D. K.; Ghosh, T.; Kandpal, S.; Tanwar, M.; Rani, C.; Kumar, R. Prussian Blue-Cobalt Oxide Double Layer for Efficient All-Inorganic Multicolor Electrochromic Device. *ACS Appl. Electron. Mater.* **2020**, *2* (6), 1768–1773. https://doi.org/10.1021/acsaelm.0c00342.

(3) *Fabrication and optimization of efficient electrochromic electrodes and devices*. https://scholar.google.com/citations?view_op=view_citation&hl=en&user=Rh4DT94AAAAJ&sortby=pubdate&citation_for_view=Rh4DT94AAAAJ:4JMBOYKVnBMC (accessed 2024-05-14).

(4) Reynolds, J. R. Electrochromism and Electrochromic Devices. By P. M. S. Monk, R. J. Mortimer and D. R. Rosseinsky. *Angew. Chem. Int. Ed.* **2008**, *47* (37), 6945–6946. https://doi.org/10.1002/anie.200785583.

(5) Wu, C.; Qiao, X.; Chen, J.; Wang, H.; Tan, F.; Li, S. A Novel Chemical Route to Prepare ZnO Nanoparticles. *Mater. Lett.* **2006**, *60* (15), 1828–1832. https://doi.org/10.1016/j.matlet.2005.12.046.

(6) Wang, M.; Jiang, L.; Kim, E. J.; Hahn, S. H. Electronic Structure and Optical Properties of Zn(OH)2: LDA+U Calculations and Intense Yellow Luminescence. *RSC Adv.* **2015**, *5* (106), 87496–87503. https://doi.org/10.1039/C5RA17024A.
(7) Sahu, B.; Bansal, L.; Ghosh, T.; Kandpal, S.; Rath, D. K.; Rani, C.; Wesemann, C.; Bigall, N. C.; Kumar, R. Metal Oxide-Mixed Polymer-Based Hybrid Electrochromic Supercapacitor: Improved Efficiency and Dual Band Switching. *J. Phys. Appl. Phys.* **2024**, *57* (24), 245110. https://doi.org/10.1088/1361-6463/ad2dba.
(8) Mishra, S.; Yogi, P.; Sagdeo, P. R.; Kumar, R. TiO2–Co3O4 Core–Shell Nanorods: Bifunctional Role in Better Energy Storage and Electrochromism. *ACS Appl. Energy Mater.* **2018**, *1* (2), 790–798. https://doi.org/10.1021/acsaem.7b00254.
(9) Bansal, L.; Ghosh, T.; Kandpal, S.; Rani, C.; Sahu, B.; Kumar Rath, D.; Wesemann, C.; Chhoker, S.; C. Bigall, N.; Kumar, R. Fluorane Sensitive Supercapacitive Microcrystalline MoO 3 : Dual Application in Energy Storage and HF Detection. *Mater. Adv.* **2023**, *4* (20), 4775–4783. https://doi.org/10.1039/D3MA00357D.
(10) PubChem. *Ethyl viologen diperchlorate*. https://pubchem.ncbi.nlm.nih.gov/compound/16212420 (accessed 2024-05-14).
(11) Ghosh, T.; Kandpal, S.; Rani, C.; Bansal, L.; Tanwar, M.; Kumar, R. Multiwavelength Color Switching from Polyaniline-Viologen Bilayer: Inching toward Versatile All-Organic Flexible Electrochromic Device. *Adv. Electron. Mater.* **2023**, *9* (2), 2201042. https://doi.org/10.1002/aelm.202201042.
(12) Mishra, S.; Yogi, P.; Chaudhary, A.; Pathak, D. K.; Saxena, S. K.; Krylov, A. S.; Sagdeo, P. R.; Kumar, R. Understanding Perceived Color through Gradual Spectroscopic Variations in Electrochromism. *Indian J. Phys.* **2019**, *93* (7), 927–933. https://doi.org/10.1007/s12648-018-1353-7.
(13) Mishra, S.; Yogi, P.; Chaudhary, A.; Pathak, D. K.; Saxena, S. K.; Krylov, A. S.; Sagdeo, P. R.; Kumar, R. Understanding Perceived Color through Gradual Spectroscopic Variations in Electrochromism. *Indian J. Phys.* **2019**, *93* (7), 927–933. https://doi.org/10.1007/s12648-018-1353-7.
(14) Poelking, C.; Daoulas, K.; Troisi, A.; Andrienko, D. Morphology and Charge Transport in P3HT: A Theorist's Perspective. In *P3HT Revisited – From Molecular Scale to Solar Cell Devices*; Ludwigs, S., Ed.; Springer: Berlin, Heidelberg, 2014; pp 139–180. https://doi.org/10.1007/12_2014_277.
(15) Kleinschmidt, A. T.; Root, S. E.; Lipomi, D. J. Poly(3-Hexylthiophene) (P3HT): Fruit Fly or Outlier in Organic Solar Cell Research? *J. Mater. Chem. A* **2017**, *5* (23), 11396–11400. https://doi.org/10.1039/C6TA08317J.
(16) Davis, K.; Yarbrough, R.; Froeschle, M.; White, J.; Rathnayake, H. Band Gap Engineered Zinc Oxide Nanostructures via a Sol–Gel Synthesis of Solvent Driven Shape-Controlled Crystal Growth. *RSC Adv.* **2019**, *9* (26), 14638–14648. https://doi.org/10.1039/C9RA02091H.
(17) Cheng, L.; Zhu, S.; Zheng, W.; Huang, F. Ultra-Wide Spectral Range (0.4–8 Mm) Transparent Conductive ZnO Bulk Single Crystals: A Leading Runner for Mid-Infrared Optoelectronics. *Mater. Today Phys.* **2020**, *14*, 100244. https://doi.org/10.1016/j.mtphys.2020.100244.
(18) Prashanth, G. K.; Dileep, M. S.; Gadewar, M.; Ghosh, M. K.; Rao, S.; Giresha, A. S.; Prashanth, P. A.; Swamy, M. M.; Yatish, K. V.; Mutthuraju, M. Zinc Oxide Nanostructures: Illuminating the Potential in Biomedical Applications: A Brief Overview. *BioNanoScience* **2024**. https://doi.org/10.1007/s12668-024-01366-4.
(19) *Thermoelectric, Electrochemical, & Dielectric Properties of Four ZnO Nanostructures - PMC*. https://www.ncbi.nlm.nih.gov/pmc/articles/PMC9784509/ (accessed 2024-05-14).

(20) Puspasari, V.; Ridhova, A.; Hermawan, A.; Amal, M. I.; Khan, M. M. ZnO-Based Antimicrobial Coatings for Biomedical Applications. *Bioprocess Biosyst. Eng.* **2022**, *45* (9), 1421–1445. https://doi.org/10.1007/s00449-022-02733-9.
(21) Šćepanović, M.; Grujić-Brojčin, M.; Vojisavljević, K.; Bernik, S.; Srećković, T. Raman Study of Structural Disorder in ZnO Nanopowders. *J. Raman Spectrosc.* **2010**, *41* (9), 914–921. https://doi.org/10.1002/jrs.2546.
(22) Talam, S.; Karumuri, S. R.; Gunnam, N. Synthesis, Characterization, and Spectroscopic Properties of ZnO Nanoparticles. *Int. Sch. Res. Not.* **2012**, *2012*, e372505. https://doi.org/10.5402/2012/372505.
(23) Raoufi, D. Synthesis and Photoluminescence Characterization of ZnO Nanoparticles. *J. Lumin.* **2013**, *134*, 213–219. https://doi.org/10.1016/j.jlumin.2012.08.045.
(24) Fatin, S. O.; Lim, H. N.; Tan, W. T.; Huang, N. M. Comparison of Photocatalytic Activity and Cyclic Voltammetry of Zinc Oxide and Titanium Dioxide Nanoparticles toward Degradation of Methylene Blue. *Int. J. Electrochem. Sci.* **2012**, *7* (10), 9074–9084. https://doi.org/10.1016/S1452-3981(23)16181-5.
(25) Novak, T. G.; Kim, J.; DeSario, P. A.; Jeon, S. Synthesis and Applications of WO3 Nanosheets: The Importance of Phase, Stoichiometry, and Aspect Ratio. *Nanoscale Adv.* **2021**, *3* (18), 5166–5182. https://doi.org/10.1039/D1NA00384D.
(26) Guo, J.; Jia, H.; Shao, Z.; Jin, P.; Cao, X. Fast-Switching WO3-Based Electrochromic Devices: Design, Fabrication, and Applications. *Acc. Mater. Res.* **2023**, *4* (5), 438–447. https://doi.org/10.1021/accountsmr.2c00217.
(27) Bonardo, D.; Septiani, N. L. W.; Amri, F.; Estananto; Humaidi, S.; Suyatman; Yuliarto, B. Review—Recent Development of WO3 for Toxic Gas Sensors Applications. *J. Electrochem. Soc.* **2021**, *168* (10), 107502. https://doi.org/10.1149/1945-7111/ac0172.
(28) Dutta, V.; Sharma, S.; Raizada, P.; Thakur, V. K.; Khan, A. A. P.; Saini, V.; Asiri, A. M.; Singh, P. An Overview on WO3 Based Photocatalyst for Environmental Remediation. *J. Environ. Chem. Eng.* **2021**, *9* (1), 105018. https://doi.org/10.1016/j.jece.2020.105018.
(29) *Processes | Free Full-Text | The Modification of WO3 for Lithium Batteries with Nickel-Rich Ternary Cathode Materials*. https://www.mdpi.com/2227-9717/11/6/1756 (accessed 2024-05-14).
(30) Thi, M. P.; Velasco, G. Raman Study of WO3 Thin Films. *Solid State Ion.* **1984**, *14* (3), 217–220. https://doi.org/10.1016/0167-2738(84)90101-2.
(31) Ghosh, T.; Rani, C.; Kandpal, S.; Tanwar, M.; Bansal, L.; Kumar, R. Chronoamperometric Deposition of Transparent WO3 Film for Application as Power Efficient Electrochromic Auxiliary Electrode. *J. Phys. Appl. Phys.* **2022**, *55* (36), 365103. https://doi.org/10.1088/1361-6463/ac76f5.
(32) Patra, A.; Auddy, K.; Ganguli, D.; Livage, J.; Biswas, P. K. Sol–Gel Electrochromic WO3 Coatings on Glass. *Mater. Lett.* **2004**, *58* (6), 1059–1063. https://doi.org/10.1016/j.matlet.2003.07.043.
(33) Anucha, C. B.; Altin, I.; Bacaksiz, E.; Stathopoulos, V. N. Titanium Dioxide (TiO_2)-Based Photocatalyst Materials Activity Enhancement for Contaminants of Emerging Concern (CECs) Degradation: In the Light of Modification Strategies. *Chem. Eng. J. Adv.* **2022**, *10*, 100262. https://doi.org/10.1016/j.ceja.2022.100262.
(34) An, M.; Yang, Z.; Zhang, B.; Xue, B.; Xu, G.; Chen, W.; Wang, S. Construction of Biochar-Modified TiO2 Anatase-Rutile Phase S-Scheme Heterojunction for Enhanced Performance of Photocatalytic Degradation and Photocatalytic Hydrogen Evolution. *J. Environ. Chem. Eng.* **2023**, *11* (5), 110367. https://doi.org/10.1016/j.jece.2023.110367.

(35) *Titanium Dioxide - TiO2 Pigment for Paint, Coatings & Inks*. https://coatings.specialchem.com/selection-guide/titanium-dioxide (accessed 2024-05-14).
(36) Melendres, C. A.; Narayanasamy, A.; Maroni, V. A.; Siegel, R. W. Raman Spectroscopy of Nanophase TiO2. *J. Mater. Res.* **1989**, *4* (5), 1246–1250. https://doi.org/10.1557/JMR.1989.1246.
(37) Kibasomba, P. M.; Dhlamini, S.; Maaza, M.; Liu, C.-P.; Rashad, M. M.; Rayan, D. A.; Mwakikunga, B. W. Strain and Grain Size of TiO2 Nanoparticles from TEM, Raman Spectroscopy and XRD: The Revisiting of the Williamson-Hall Plot Method. *Results Phys.* **2018**, *9*, 628–635. https://doi.org/10.1016/j.rinp.2018.03.008.
(38) *Cyclic Voltammetry Studies of Nanoporous Semiconductors. Capacitive and Reactive Properties of Nanocrystalline TiO2 Electrodes in Aqueous Electrolyte | The Journal of Physical Chemistry B*. https://pubs.acs.org/doi/full/10.1021/jp0265182 (accessed 2024-05-14).
(39) Molybdenum Trioxide. *Wikipedia*; 2024.
(40) *High-pressure Raman scattering and x-ray diffraction of phase transitions in MoO3 | Journal of Applied Physics | AIP Publishing*. https://pubs.aip.org/aip/jap/article/105/2/023513/284245/High-pressure-Raman-scattering-and-x-ray (accessed 2024-05-14).
(41) Hsu, C.-S.; Chan, C.-C.; Huang, H.-T.; Peng, C.-H.; Hsu, W.-C. Electrochromic Properties of Nanocrystalline MoO3 Thin Films. *Thin Solid Films* **2008**, *516* (15), 4839–4844. https://doi.org/10.1016/j.tsf.2007.09.019.
(42) *Electrochemical Impedance Spectroscopy─A Tutorial | ACS Measurement Science Au*. https://pubs.acs.org/doi/10.1021/acsmeasuresciau.2c00070?ref=PDF (accessed 2024-05-14).